

MIT OpenCourseWare  
<http://ocw.mit.edu>

12.740 Paleoceanography  
Spring 2008

For information about citing these materials or our Terms of Use, visit: <http://ocw.mit.edu/terms>.

Glacial/Interglacial 'oscillations': WHY?  
Time-series analysis

12.740 Lecture 4 Spring 2008

# SPECMAP 150 ka indicators

Image removed due to copyright restrictions.

We now understand how climate has changed over the past few  $10^5$  years. Similar basic patterns are seen in most indicators (with a few loose ends). We can begin to ask the question: Why?

- Two approaches:

1. "The physics": derive ice ages from first principles. Good luck! (call me when you get there).

2. "Correlation (not causation)": look for similarities (coincidences?) between certain driving forces known from first principles and the climate record. Examine the odds that such a correspondence is due to chance. If the odds are good, look into the relevant mechanism in more detail. To be successful, this approach needs: (1) reliable climate record not excessively modified by bioturbation; (2) but the record also needs to be reasonably long so that many cycles are available for statistical tests. Must compromise here! Eventually need to come to an accommodation with "the physics".

# History:

- ~1840: Agassiz proposed massive continental glaciation; debate ensued which eventually was decided in his favor
- ~1860: Croll proposed that changes in the earth's orbital parameters were responsible for glaciation. Theory received a mixed reception.
- ~1920 Milankovitch undertook detailed calculations which quantified the expected variations in the earth's orbital parameter and proposed that summer insolation at  $65^{\circ}\text{N}$  was the key [more or less summer insolation  $\Rightarrow$  more or less glacial melting]. Theory encountered a mixed reception.
- 1950's: Emiliani found stronger evidence for cyclic oscillations; tried to revive Milankovitch. Problem: time scale.
- 1960's, 70's: Barbados data (and hence correct time scale) revived interest in Milankovitch hypothesis. Theory was being taken seriously, but it was considered far from proven.
- 1976: Hays, Imbrie, Shackleton paper. Overcame most of the resistance to some degree of orbital influence over climate (at least as a "pacemaker" of ice ages).

At present, relatively few people doubt that insolation changes play a role in climate change, but there are reasonable questions as to their importance relative to other factors. Even: to what extent is climate actually predictable? Are there significant internal resonances that interact with orbital forcing? What is the origin of large amplitude sub-orbital climate variability? Can we parlay our understanding of past climate change into better predictions of future climate change?

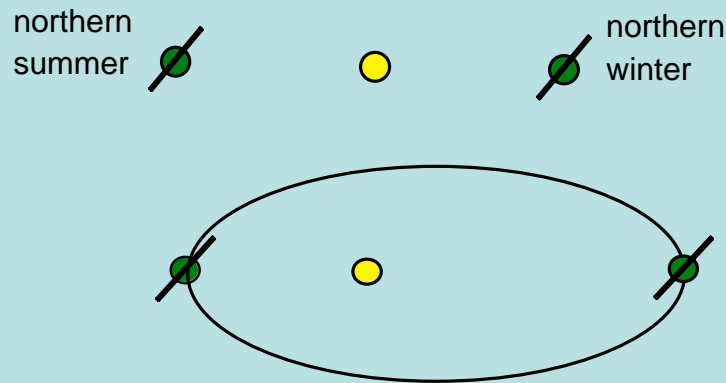
Climate models incorporate a lot of first principle physics (e.g. laws of motion, radiation physics, and thermodynamics), but because of the enormous complexity of the system and limited computer capabilities, these models contain less definitive representations of sub-grid scale processes and of poorly understood processes (e.g. convective precipitation and clouds; sea ice formation and melting; relation between soil, vegetation, evaporation, precipitation and river runoff). In the aggregate, these factors are extremely important, so they cannot be left out. Instead they are handled by empirical parameterizations containing "fudge factors" which are "tuned" to give a reasonable representation of modern climate. This approach is OK for weather forecasting, because many of these factors can't change fast enough to effect tomorrow's weather. But for climate change, these uncertainties are a serious problem. The sensitivity of the models to various forcing factors might be seriously misestimated by these parameterizations. One way to test the sensitivity of these models is to see how they behave when driven by well-known forcing functions (e.g. a recent volcanic eruption). One of the best known forcing functions linked to large climate change is the effect of the earth's orbital parameters on incoming radiation.

# Changes in the earth's orbital parameters and their influence on radiation receipt at the top of the atmosphere I

Root cause: gravitational interaction between the earth with the sun and other planets. Precession changes are caused by angular momentum and the gravitational field of the Sun; tilt/eccentricity variations due (mainly) to Sun-Jupiter tug-of-war for the earth.

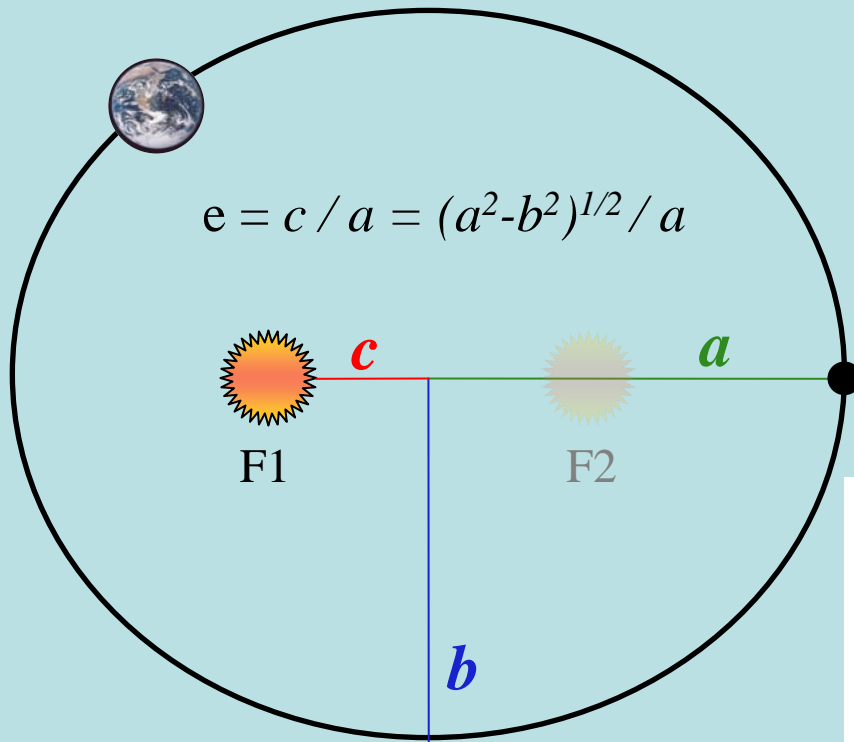
The seasons result from the tilt of the earth's axis relative to the plane of the orbit (view from plane of orbit:

Edge plane view (circular orbit):

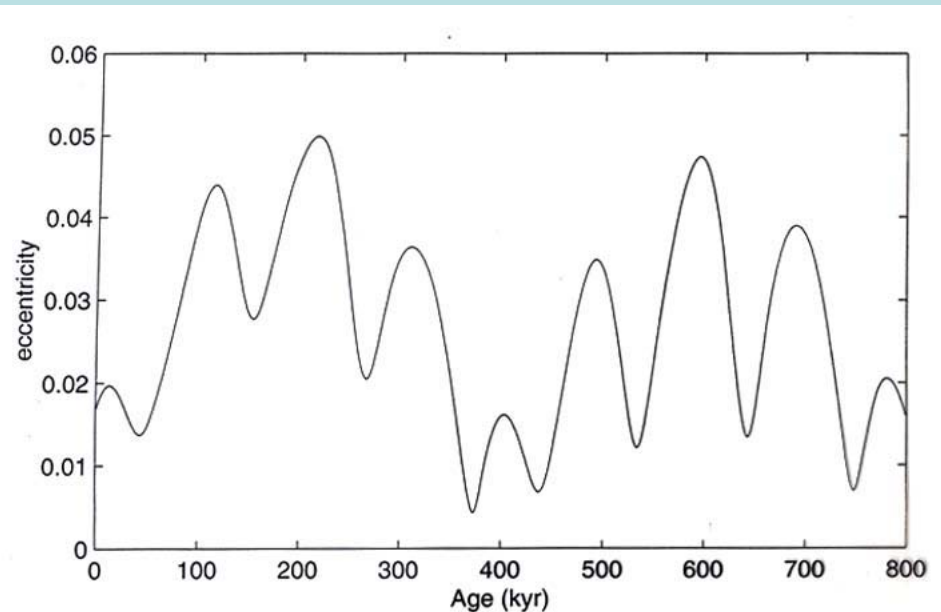


Oblique view, with exaggerated eccentricity

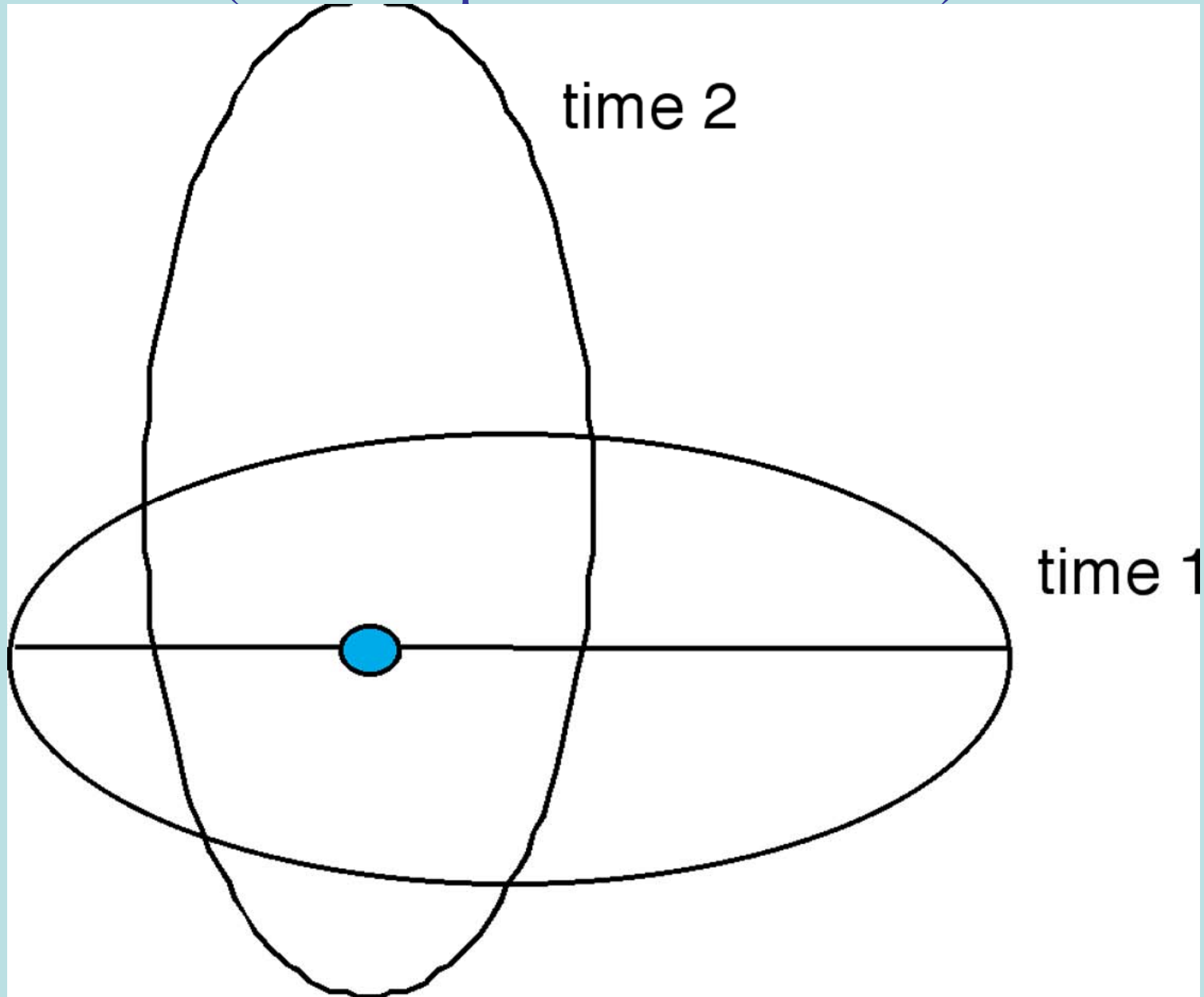
# Eccentricity of Present Earth Orbit Around Sun (to Scale)



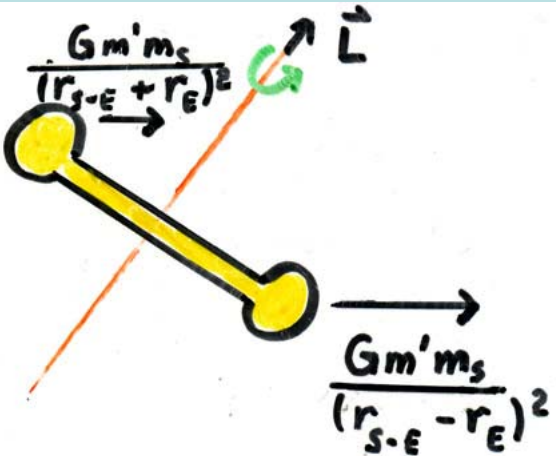
Present eccentricity = 0.017  
Range: 0 - 0.06  
100 & 400 kyr periods



# Precession of elliptical orbit (with respect to fixed stars)



# Precession



Precession frequency depends on angular momentum and torque

$$P = 25,700 \text{ years}$$

Eccentricity amplitude-modulates precession parameter

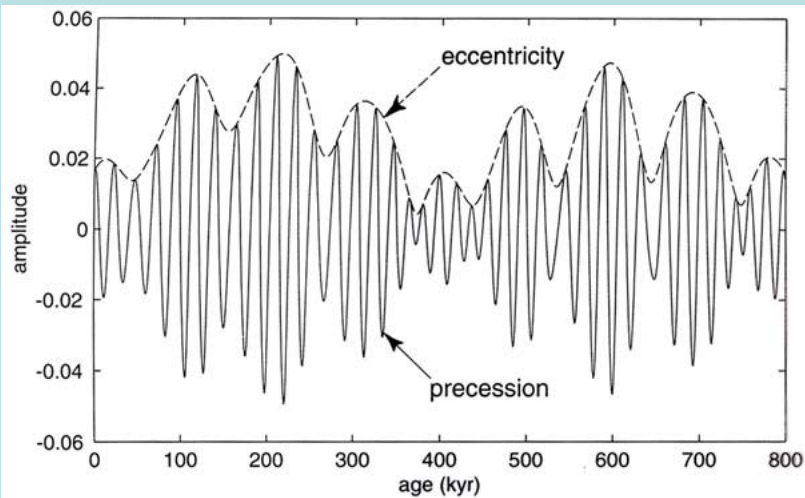
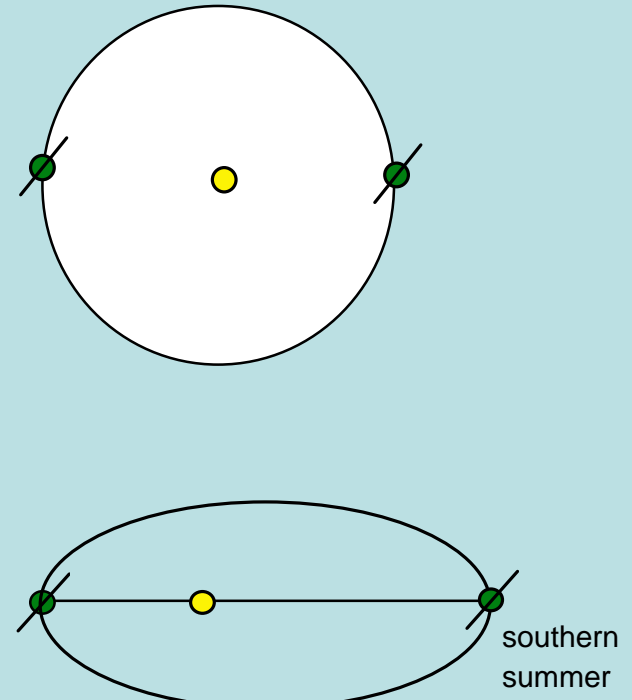


Fig. 2.10. Precession parameter  $p$  and eccentricity.

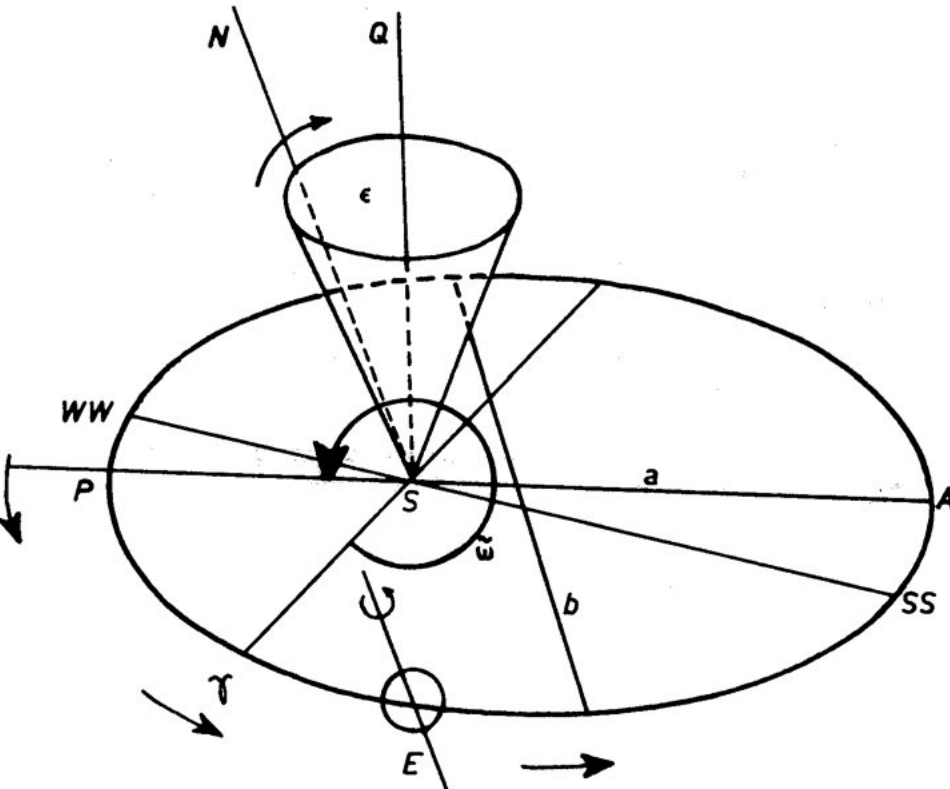
$$p = e \sin \omega$$

$\omega$   $\angle$  between Spring Equinox + perihelion



# Elements of the Earth's Orbit

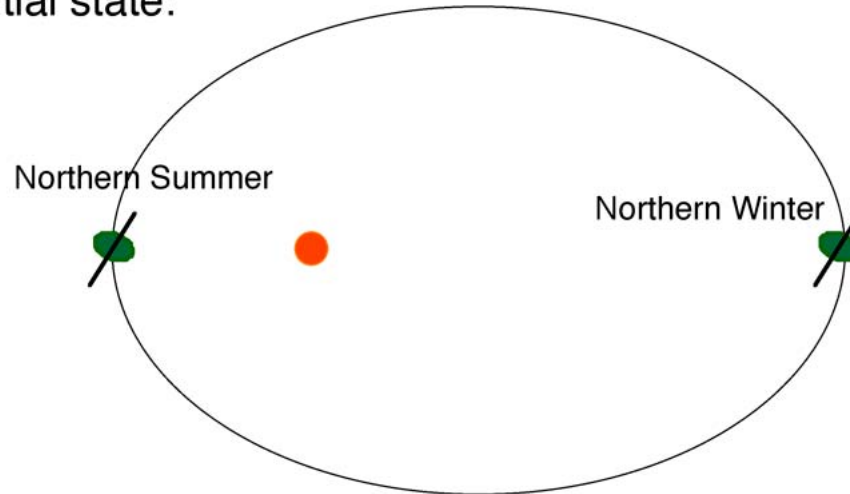
(Berger, 1981)



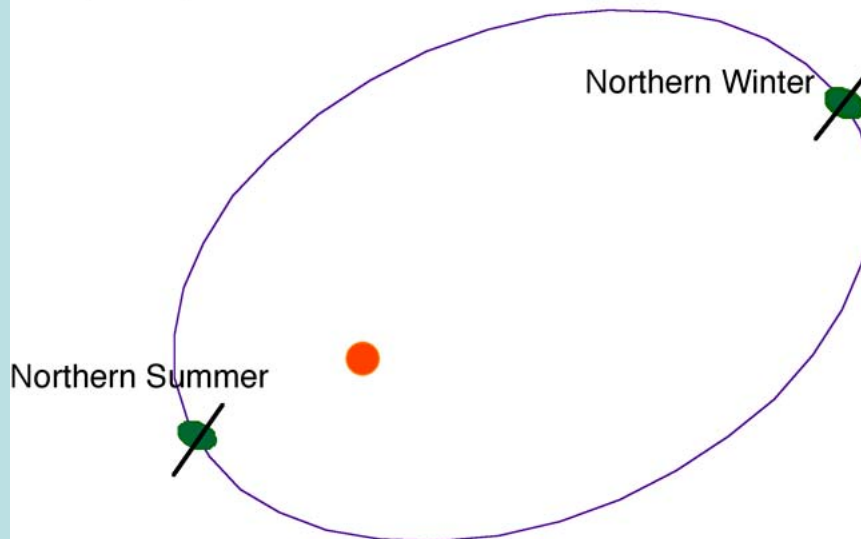
Elements of the earth's orbit. The orbit of the Earth E, around the Sun S is represented by the ellipse P  $\gamma$  E A, P being the perihelion and A the aphelion. Its eccentricity  $e$ , is given by  $(a^2 - b^2)^{1/2} / a$ ,  $a$  being the semimajor axis and  $b$  the semiminor axis. WW and SS are respectively the winter and the summer solstice,  $\gamma$  is the vernal equinox; WW, SS and  $\gamma$  are located where they are today. SQ is perpendicular to the ecliptic and the obliquity,  $\epsilon$ , is the inclination of the equator upon the ecliptic, i.e.  $\epsilon$  is equal to the angle between the earth's axis of rotation SN and SQ.  $\omega$  is the longitude of the perihelion relatively to the moving vernal equinox and is equal to  $\Pi + \psi$ . The annual general precession in longitude,  $\psi$ , describes the absolute motion of  $\gamma$  along the earth's orbit relative to the fixed stars.  $\Pi$ , the longitude of the perihelion, is measured from the reference vernal equinox of 1950 A.D. and describes the absolute motion of the perihelion relatively to the fixed stars. For any numerical value of  $\omega$ ,  $180^\circ$  is subtracted for a practical purpose: observations are made from the Earth, and the Sun is considered as revolving around the Earth.

# Precession influence on climate: why 23,000 years not 25,800?

Initial state:



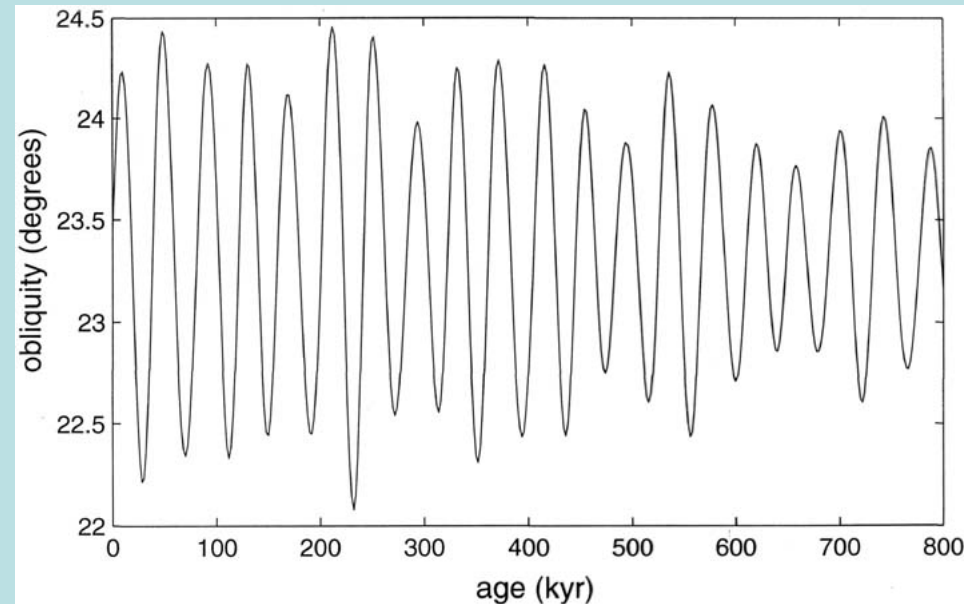
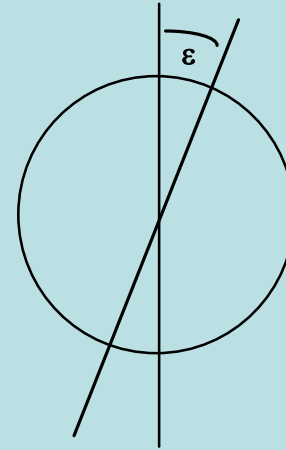
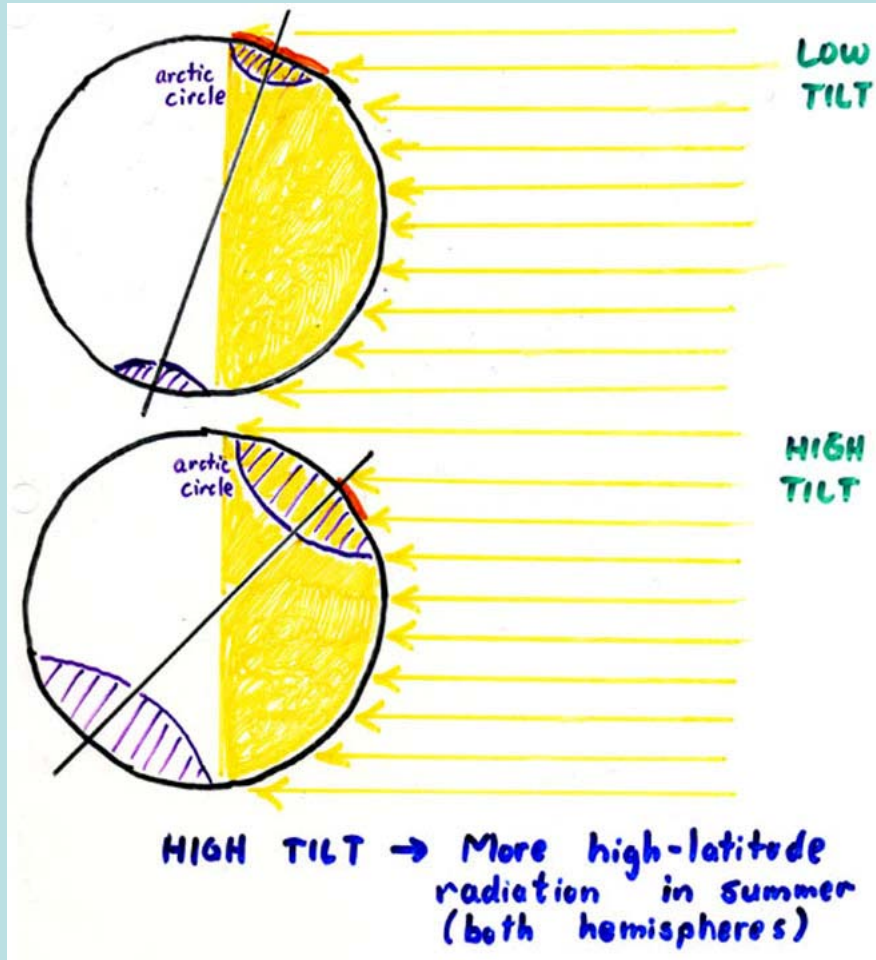
~22,000 years later:



Earth's axis has precessed 22/26 of a cycle, and the eccentricity of the orbit has precessed "backwards" 4/26 of a cycle, bringing us back to a configuration which is equivalent in terms of radiation

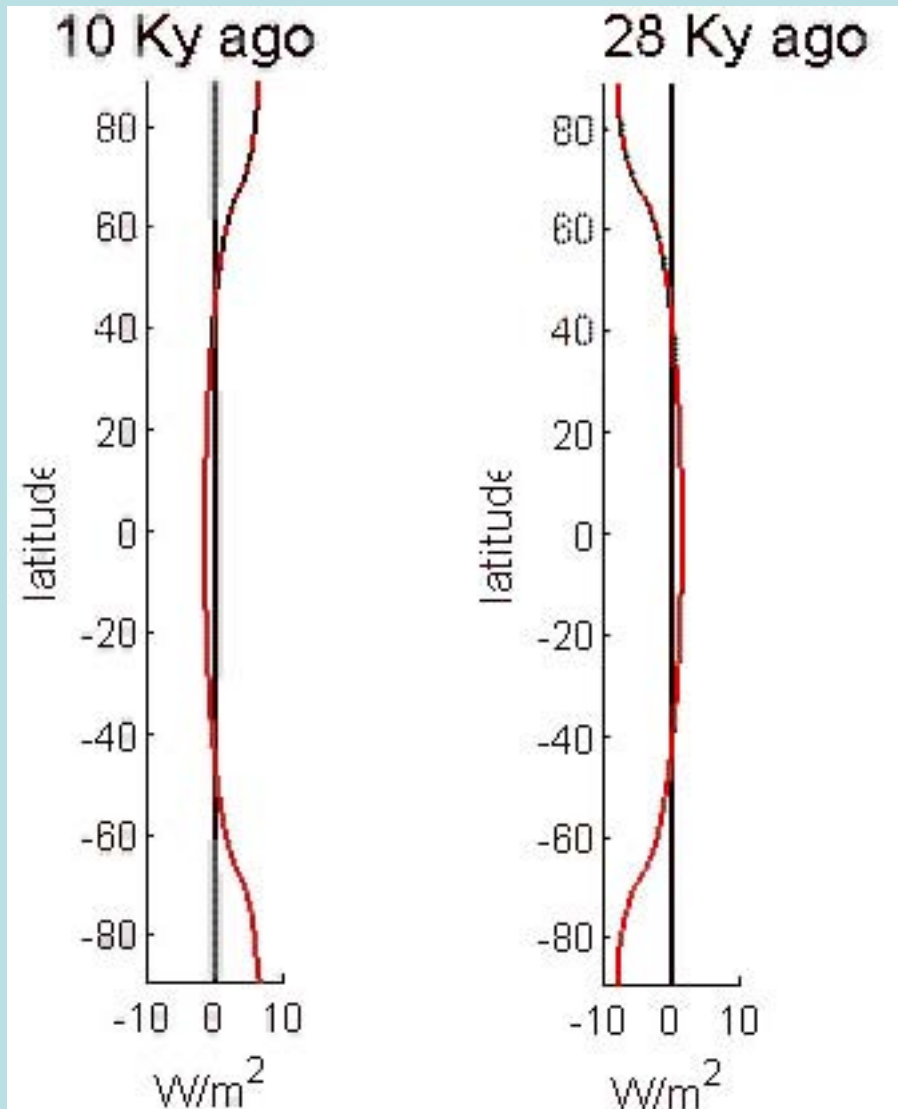
# Obliquity (tilt)

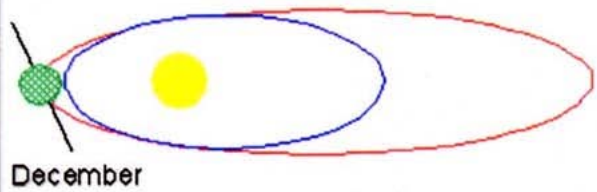
Obliquity varies between  $\sim 21.8^\circ$  and  $24.4^\circ$ ; at present the obliquity is  $23.44^\circ$ . Affects the latitude of the tropics and the arctic circle. Period is  $\sim 41,000$  years, and is relatively regular. Think of this as part of a solar system angular momentum oscillator (angular momentum conserved in solar system, but with transfers between objects)



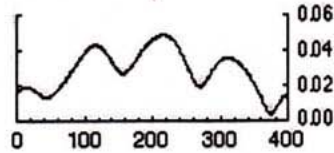
Higher obliquity leads to higher summer insolation at high latitudes (and slightly less at low latitudes).

Obliquity change re-apportions radiation between polar regions and tropics

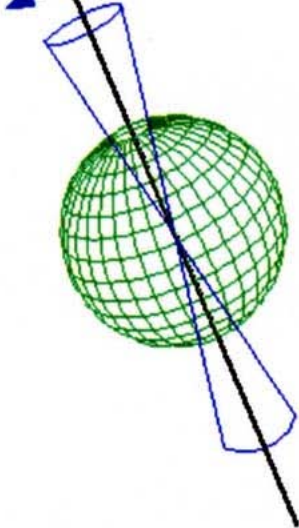




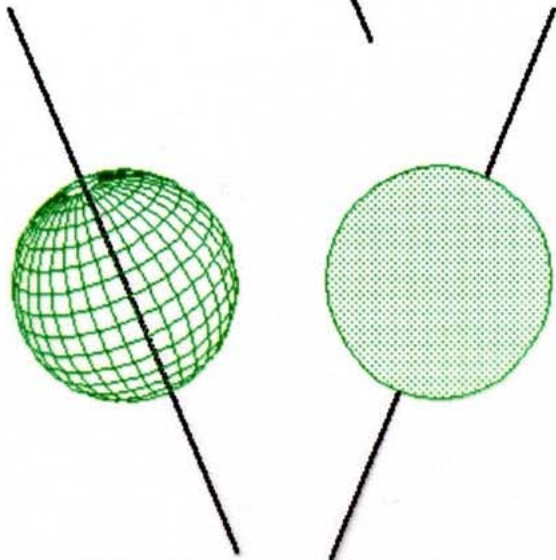
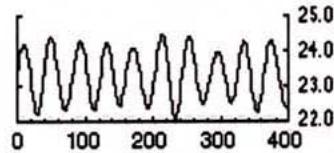
Eccentricity: 100 kyr



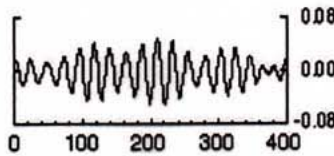
$23.5 \pm 1^\circ$



Tilt: 41 kyr

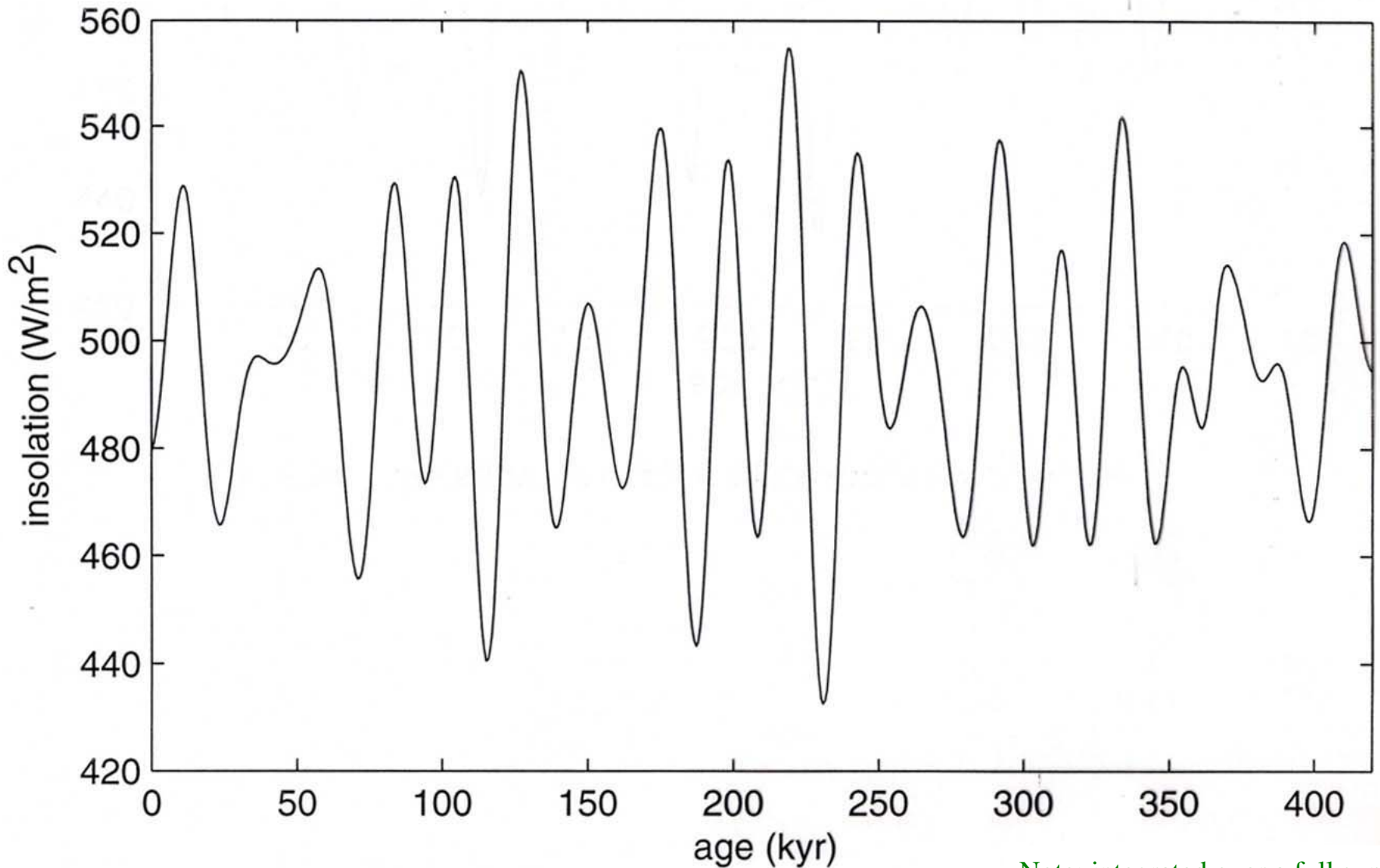


Precession: 23-19 kyr



Periodic changes in orbital geometry modulate solar radiation receipts (insolation)

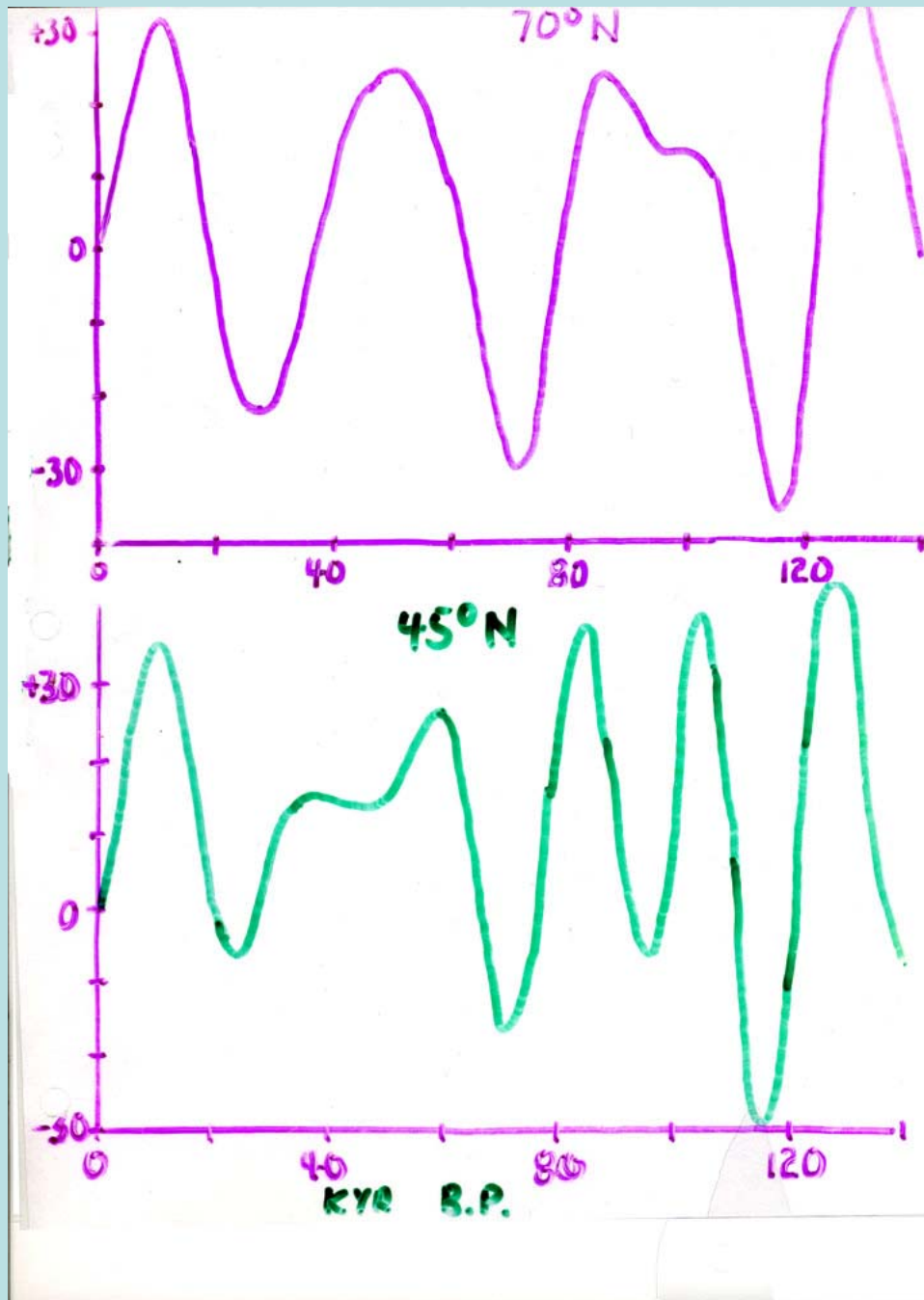
# Insolation at 65°N, “June 21”



Insolation, July 65N.

Note: integrated over a full summer-centered half year, effect of obliquity is stronger at high latitudes

Summer half-year insolation, cal/cm<sup>2</sup>/day



Integrated over a half-year centered on summer, obliquity dominates high latitude insolation and precession dominates lower latitude insolation

## Summary: orbital influence on insolation at the top of the atmosphere

- These changes in the earth's orbital elements affect radiation received at the top of the atmosphere ("insolation") as a function of hemisphere, latitude, and time of year.

Effect of precession/eccentricity:

Inter-hemispheric radiation receipt: the hemisphere whose summer occurs during perihelion receives more insolation than the other hemisphere). The higher the eccentricity, the stronger the contrast.

Seasonal contrast within a hemisphere: as a hemisphere alternates between periods of summer perihelion and winter perihelion, the seasonal contrast in insolation is modified. The two hemispheres are out of phase with respect to this effect.

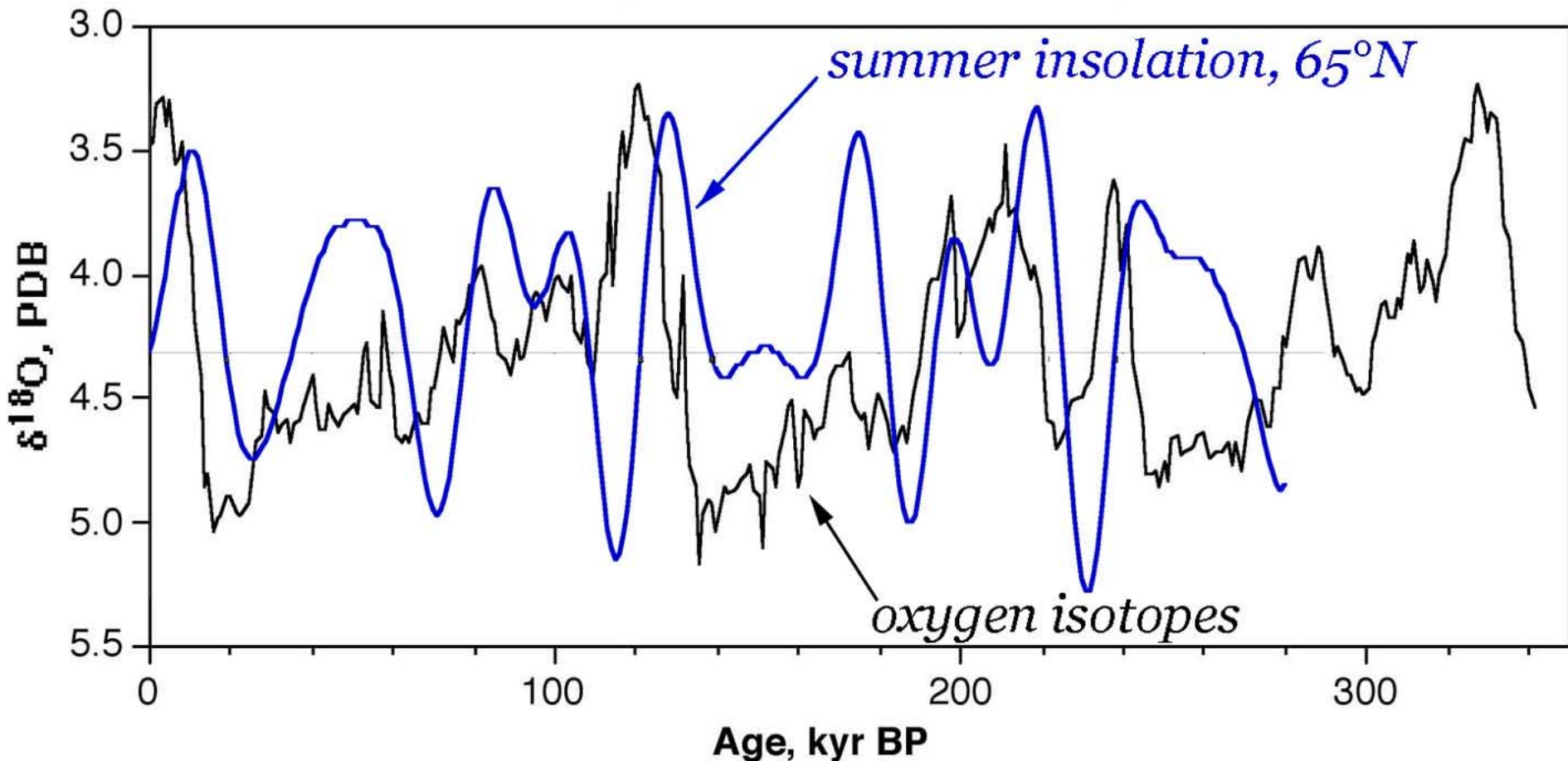
Effect of obliquity: high-latitude summer insolation: high tilt leads to more radiation received at high latitudes during summer (that comes at the expense of the mid- and low-latitudes; high-latitude winters not affected by changes in tilt).

- These orbital characteristics can all be calculated accurately via Newtonian mechanics into the distant past (many millions of years). Accumulation of uncertainties (e.g. in relative masses of planets; shape and density distribution of planets) causes absolute values (i.e., which side of the sun is the earth on at some exact point in time in the future?) to be uncertain beyond several million years, although the frequencies are probably known reasonably well beyond that time. For the last million years, we may regard these calculations as virtually unquestionable.

How do we make the comparison between these precisely calculable orbital changes and the record of climate change?

- Curve-matching is always popular. But given subjectivity, the possibility of phase lags, and a rubber time scale, this approach has drawbacks.
- Objective methods: many are possible, but for cyclic processes, Fourier analysis is a natural. It is nonetheless possible to be fool oneself with it's mathematical elegance, however; the statistics assume certain characteristics that might not apply to the data at hand.

# Oxygen isotopes compared to summer insolation at 65°N



# Fourier time-series analysis

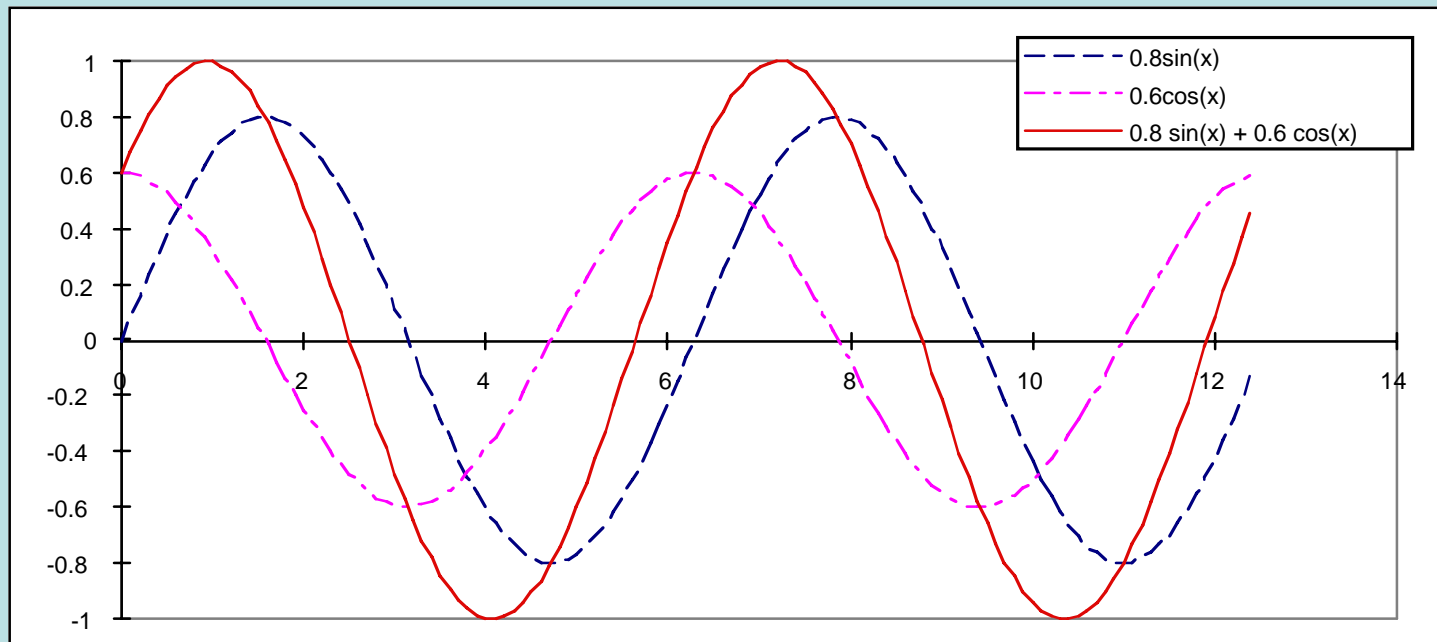
- Prism analogy: look at component frequencies of a time-variant process. Fourier showed that any reasonable function of time can be represented as a sum of sines & cosines.
- Theorem: Let  $G(t)$  be any well-behaved (continuous; differentiable; continuous derivatives) function. If we sample this function discretely in uniform time intervals (creating a series  $G(t_1), G(t_2), \dots, G(t_n)$ ), then there is one (and only one) complex function  $S(f) = A(f) + iB(f)$  [where  $s$  is frequency,  $t_n$  is the record length and  $i$  is the square root of  $-1$ ] such that
  - $$G(t) = \sum (a_j \sin f_j + b_j \cos f_j)$$
  - where  $f_j = j/t_n$  for  $j = 1 \dots n$
  - These harmonics  $f_j$  are orthogonal (i.e. one cannot reconstruct  $f_j$  wave as  $\sum_{k \neq j} f_k$  waves and the harmonics  $f_j$  are complete (i.e. any "reasonable" signal in  $t$  can be fit perfectly & uniquely).
    - This is the discrete Fourier Transform

# Formal definition of the Fourier Transform

$$S(f) = \int_{-\infty}^{+\infty} G(t) e^{-i\omega t} dt$$

where  $\omega = 2\pi f$

Complex short-hand:  $e^{iy} = \cos y + i \sin y$



The Fourier Transform is reversible:

$$G(t) = \int_{-\infty}^{+\infty} S(f) e^{i\omega f} df$$

The Fourier Transform of a single sine wave is a spike at a single frequency. Similarly, the Inverse Fourier Transform of a single spike frequency is a sine wave.

# Computation of the Fourier Transform

Accepting the truth of the theorem, the discrete Fourier Transform is just an application of simultaneous equations. For discrete uniformly-sampled data, we are taking  $N$  observations of  $G(t)$  from  $t_1$  to  $t_N$  [whose record length (period) is  $P=t_N-t_1$ ] and the spacing between samples is  $\Delta t=P/(N-1)$ ] and converting to  $N/2$  pairs of sine and cosine coefficients. The number of coefficients is equal to the number of observations, so this is an exercise in solving a system of  $N$  simultaneous equations. Let  $\mathbf{A}$  = an  $N \times N$  square array of the sine and cosine time series for each of the harmonics, where each row  $n$  of the array (for  $j= 0$  to  $N-1$ ) is:

$$\begin{matrix} \sin(2\pi j\Delta t) & \cos(2\pi j\Delta t) & \sin(4\pi j\Delta t) & \cos(4\pi j\Delta t) & \sin(6\pi j\Delta t) & \cos(6\pi j\Delta t) & \dots & \sin(2\pi(N/2) j\Delta t) & \cos(2\pi(N/2) j\Delta t) \end{matrix}$$

e.g.:

$$\mathbf{A} = \begin{bmatrix} \sin(2\pi/N 0*\Delta t) & \cos(2\pi/N 0*\Delta t) & \sin(4\pi/N 0*\Delta t) & \cos(4\pi/N 0*\Delta t) & \dots & \sin(2\pi(N/2) 0*\Delta t) & \cos(2\pi(N/2) 0*\Delta t) \\ \sin(2\pi/N 1*\Delta t) & \cos(2\pi/N 1*\Delta t) & \sin(4\pi/N 1*\Delta t) & \cos(4\pi/N 1*\Delta t) & \dots & \sin(2\pi(N/2) 1*\Delta t) & \cos(2\pi(N/2) 1*\Delta t) \\ \dots & \dots & \dots & \dots & \dots & \dots & \dots \\ \sin(2\pi/N (N-1)\Delta t) & \cos(2\pi/N (N-1)\Delta t) & \sin(4\pi/N (N-1)\Delta t) & \cos(4\pi/N (N-1)\Delta t) & \dots & \sin(2\pi(N/2) (N-1)\Delta t) & \cos(2\pi(N/2) (N-1)\Delta t) \\ \dots & \dots & \dots & \dots & \dots & \dots & \dots \end{bmatrix}$$

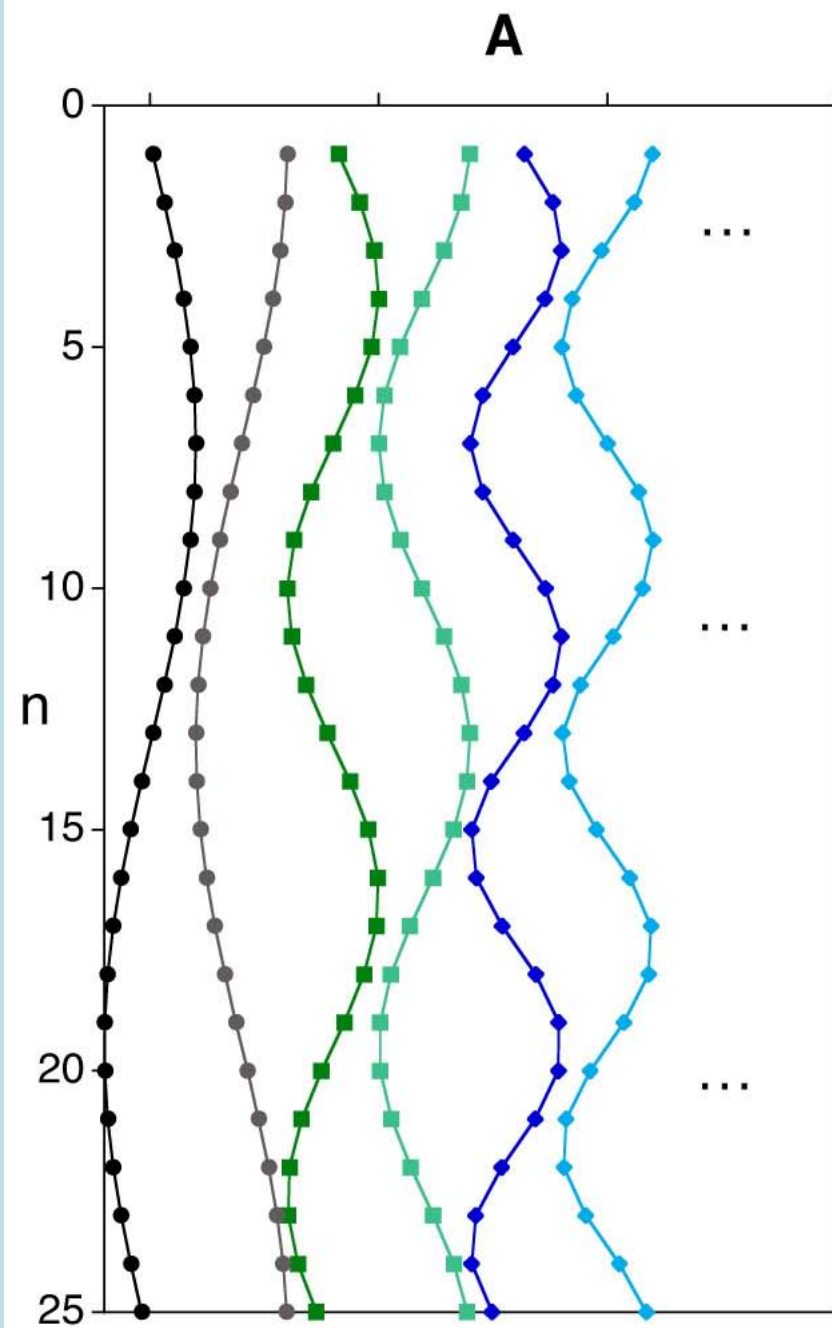
and let  $\mathbf{x}$  = an  $N \times 1$  vector of the Fourier coefficients (a, b) arranged vertically:

$$\mathbf{x} = \begin{bmatrix} a_1 \\ b_1 \\ a_2 \\ b_2 \\ \dots \\ a_{N/2} \\ b_{N/2} \end{bmatrix}$$

and let  $\mathbf{g}$  = an  $N \times 1$  vector of the discrete observations of  $G(t)$ :

$$\mathbf{g} = \begin{bmatrix} g(t_1) \\ g(t_2) \\ g(t_3) \\ g(t_4) \\ \dots \\ g(t_{N-1}) \\ g(t_N) \end{bmatrix}$$

So:  $\mathbf{Ax} = \mathbf{G}$



$x$

$=$

$g$

$a_1$

$b_1$

$a_2$

$b_2$

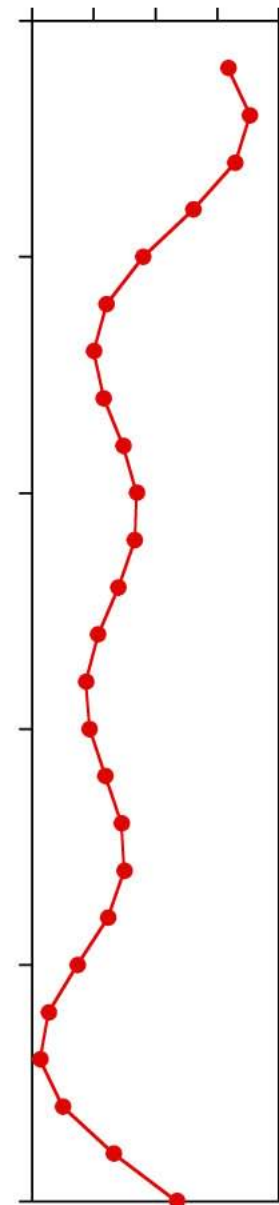
$a_3$

$b_3$

...

$a_{N/2}$

$b_{N/2}$



# Solution to the simultaneous equations

Because the Fourier Transform theorem says:

$$(a) \mathbf{g} = \mathbf{A} \mathbf{x}$$

then the Fourier coefficients are given by the simultaneous equations matrix solution:

$$(b) \mathbf{x} = \mathbf{A}^{-1} \mathbf{g}$$

(You might wonder if the rows must be linearly independent, ensuring that the inverse of  $\mathbf{A}$  exists. In effect, the Fourier theorem is a statement that they must be, for "reasonable" time series functions)

The above method is one way to calculate the Fourier transform. However, the fastest, most efficient route is the Fast Fourier Transform (FFT). This is a simple routine which calculates the solution to the series of simultaneous equations in a highly efficient way. It occupies about 64 lines of a BASIC program; see "The Visible FFT" spreadsheet to understand the algorithm). Typically, you either interpolate your data to give a series with a power of two of evenly spaced (in time) data points (which usually makes sense because paleoclimatic data sets are usually unevenly spaced in time), or add "trailing zeroes" to your data set until you reach a power of two.

Older papers use the method of "Blackman and Tukey" which was developed before the FFT. It was commonly used throughout the SPECMAP project. It is based on the "autocorrelation" technique, which involves calculating the correlation coefficient of a time series relative to itself (autocorrelation) after sliding the series by a variable number of "lags". The methods are mathematically equivalent, however, and the results should not depend strongly on the technique used.

# Alternative methods

Expressing the method as in the equation above points the way to alternative ways of calculating the spectra in situations involving unevenly spaced data and/or time series with gaps. In those cases, one can convert the original time series to a time series with  $\sin$ ,  $\cos$  ( $\mathbf{x}$ ) values corresponding to "times" ( $t$ ) of the individual measurements, regardless of their spacing. So the  $N$  rows in matrix  $A$  become

$$\begin{bmatrix} \sin(2\pi(t_1 - t_1)/P) & \cos(2\pi(t_1 - t_1)/P) & \sin(2*2\pi(t_1 - t_1)/P) & \cos(2*2\pi(t_1 - t_1)/P) & \dots & \sin(N*2\pi(t_1 - t_1)/P) & \cos(N*2\pi(t_1 - t_1)/P) \\ \sin(2\pi(t_2 - t_1)/P) & \cos(2\pi(t_2 - t_1)/P) & \sin(2*2\pi(t_2 - t_1)/P) & \cos(2*2\pi(t_2 - t_1)/P) & \dots & \sin(N*2\pi(t_2 - t_1)/P) & \cos(N*2\pi(t_2 - t_1)/P) \\ \dots & \dots & \dots & \dots & \dots & \dots & \dots \\ \sin(2\pi(t_N - t_1)/P) & \cos(2\pi(t_N - t_1)/P) & \sin(2*2\pi(t_N - t_1)/P) & \cos(2*2\pi(t_N - t_1)/P) & \dots & \sin(N*2\pi(t_N - t_1)/P) & \cos(N*2\pi(t_N - t_1)/P) \end{bmatrix}$$

where  $t_i$  is the time corresponding to each observation ( $t_1$  is the first observation) and  $P$  is the time length of the series of observations ( $t_N - t_1$ ).

This format can result in a situation where there are more Fourier coefficients (which must remain as the harmonics of the time series record length) than observations. This situation can be dealt with by ignoring the highest harmonics (i.e., chopping off the right hand side of the equation as necessary). In fact, it is possible to ignore most of the higher harmonics entirely [which often makes sense in paleoclimatic time series, where the error on the time scale renders the highest Fourier coefficients meaningless], resulting in a situation where there are more observations than Fourier coefficients. In this case, the equation can be solved using a least squares approach:

$$\mathbf{x} = (\mathbf{A}^T \mathbf{A})^{-1} \mathbf{A}^T \mathbf{g}$$

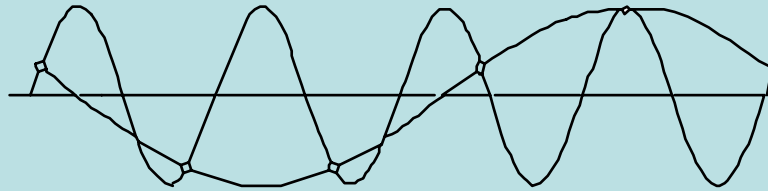
These methods aren't as computationally efficient as the FFT, but given the power of modern computers, the drain on computing power is trivial when relatively few spectra are being calculated.

FT needs “infinite data”; gets it by stacking record end-to-end repeatedly

The finite discretely sampled time series Fourier transform treats the data as though it were periodic, i.e. the measured time series repeats itself over and over again. This leads to some problems: if first and last data points are quite different, the FT must use many high-frequency harmonics of the fundamental frequency in order to create the sharp break. This problem is handled by windowing (see later)

# Nyquist Folding Frequency and Aliasing

With a fixed discrete sampling frequency, it is not possible to observe frequencies that are higher than half that sampling frequency. Even worse, the higher frequencies come back at you as if they were signals of lower frequency (aliasing):

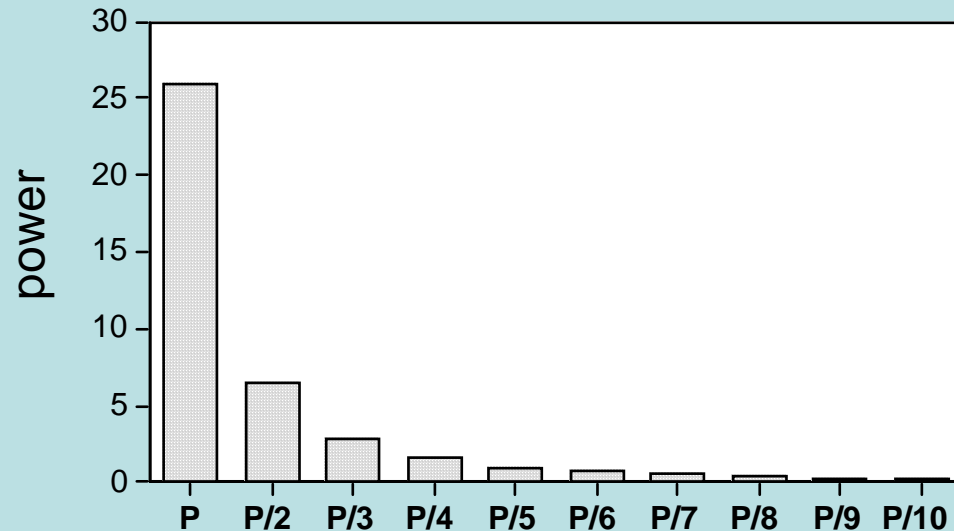
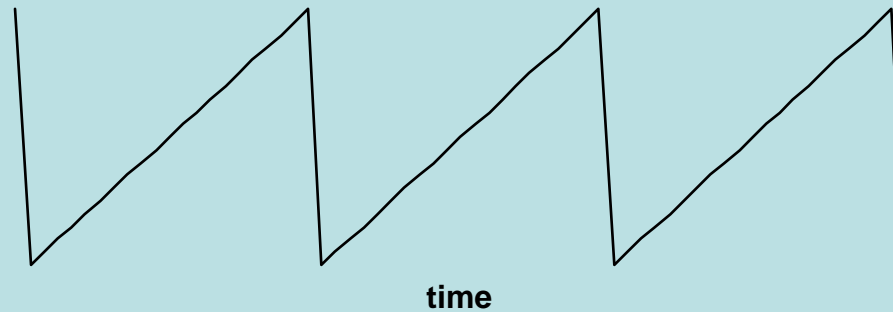


(Aliasing is the reason that the wagon wheels in old western movies look like they are moving backwards.)

This problem can be avoided by using a filter to eliminate frequencies that are higher than the Nyquist frequency (such as sampling at a very high rate and integrating the signal for the duration of the sampling interval). Bioturbation is actually helpful here - you won't find daily cycles in oxic marine sediment cores.

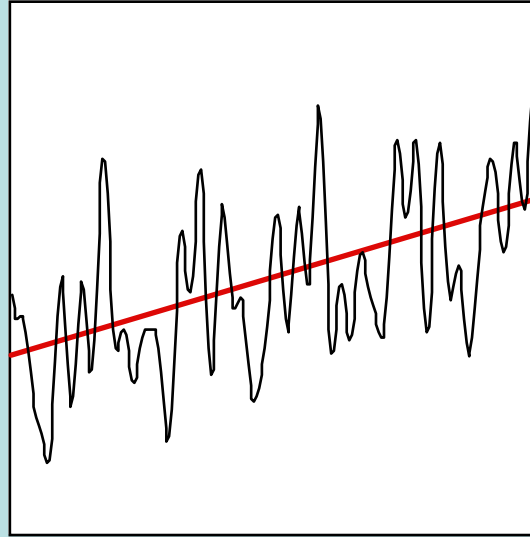
# Harmonics

The spectrum of a sawtooth (repeated linear trend) includes harmonics of the fundamental period  $P$ :



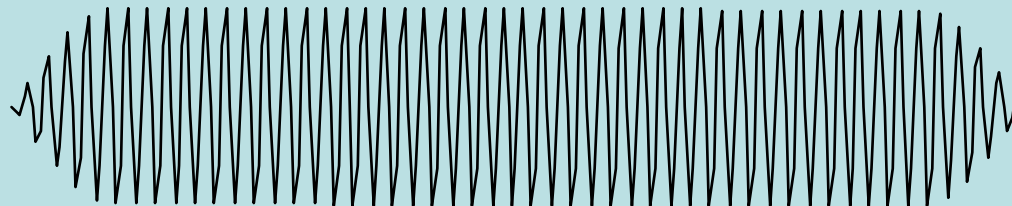
# Detrending and Tapering

Detrending: removing the long-term trend from the data (by a linear regression (or any other appropriate trend, which need not be linear)).



time

Tapering: in order to ensure that there are no abrupt mismatches between first and last data points (e.g. a glacial connecting to an interglacial with no transition), the time series can be tapered to zero at the beginning and end. For example, a "cosine bell" can be used for this purpose (a cosine maximum to minimum multiplier) for the first and last 10% of the data series. The subject of tapering is complicated, and at present it is generally agreed that the "optimal" method is David Thompson's "multitaper method", which blends the result from a family of tapers.



time

# Power Spectrum

Electrical analogy:  $\text{Power} = i^2R$

(where  $i$  = electrical current and  $R$  = resistance)

Amplitude of cycle at frequency  $j$  is  $(a_j^2 + b_j^2)^{1/2}$

(i.e., the length of the vector in (sin,cos) space,

the complex conjugate  $(a+bi)(a-bi)$

[where  $i$  is the imaginary number, square root of -1]

By analogy, then,  $a_j^2 + b_j^2 = \text{power at frequency } f_j$  (i.e., the (amplitude squared) of cycle  $j$ ).

The measurement units of power are  $\text{amplitude}^2 / (\text{cycles per time unit})$ .

# What does “power” mean for a climate time series?

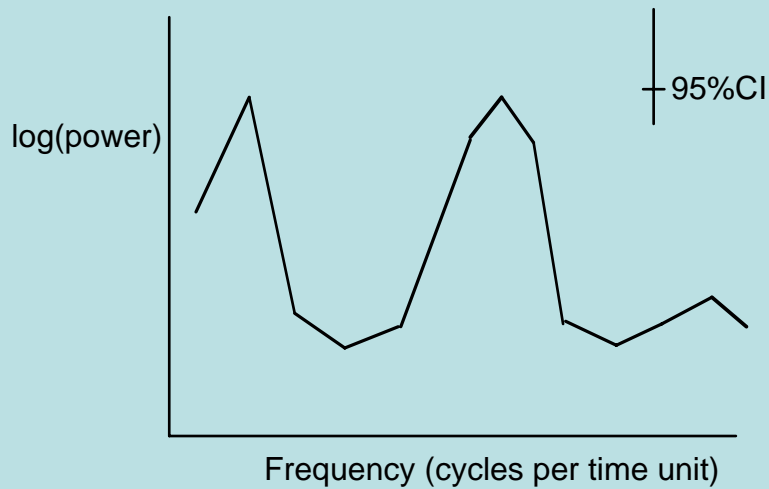
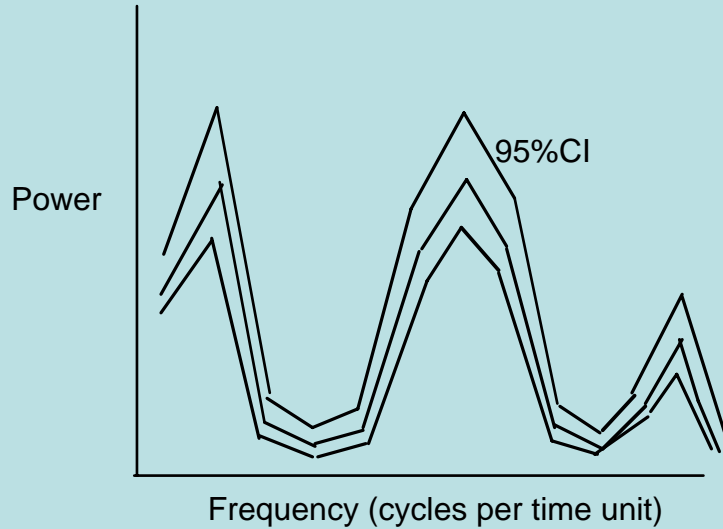
The logic behind using power spectra for climate processes is debatable. Power spectra arose in the field of electrical engineering, so the choice is obvious in that context. It is not so obvious in the case of sea level; even if you would want to know the change in gravitational potential energy due to changing sea level, it is not proportional to the square of the amplitude. Perhaps the best justification for “power” is that it is closely related to variance; many of the same mathematical concepts we use for variance statistics apply to power.

$$2 \sum (a_i^2 + b_i^2) \Delta f = \sum X_i^2$$

frequency bandwidth      data

Sometimes, it might often be more useful to present amplitude spectra, which can simply be related to the wiggles one sees in the data (e.g. meters change of sea level). Typically, this is not done, solely because of the electrical origin of spectral analysis; statistical packages usually derive spectral estimates using programs written for electrical analysis. In any event, it is straightforward to take the square root of the power to get the amplitude.

# Periodogram



The periodogram is a plot of power or  $\log_{10}(\text{power})$  vs/ frequency, which is evenly spaced for the Fourier Transform

# Statistical significance of the periodogram

White noise: equal energy (power) per frequency band  $\Delta f$  (almost equivalent to random number series in time).

Just as tossing a small number of coins is unlikely to give precisely 50% heads and tails, a finite random time series is unlikely to have precisely equal energy per  $\Delta f$ ; in effect, "counting statistics" play a role; the longer the time series, the less the fluctuations within  $\Delta f$ .

Hence, a finite time series of a non-periodic function will show peaks and valleys in the periodogram. We would like to define criteria so that we can assess the likelihood that a peak observed in a real time series is due purely to chance.

There are a number of "rules" around which purport to tell you "how many cycles" you need to prove a periodic process; typically these rules specify 5 or 10 cycles. While there is a grain of truth within these rules, they can be misleading. Is a record with only 9 cycles unconvincing yet one with 11 cycles totally convincing? The statistics follow a continuum, so there is little statistical difference in the reliability of records with 9 or 11 cycles. Perhaps a more fundamentally misleading characteristic of these "rules" is that they ignore the relationship between the cycle you are trying to see and the characteristics of the rest of the variability. A very weak cycle (which nonetheless exists) can be hidden in the "noise" of the data in the physical system; it can take many more than 10 cycles to verify the existence of a weak cycle. On the other hand, the characteristics of a very strong cycle can be estimated reliably with just a few cycles (although it is another thing to prove that those cycles couldn't have originated from chance). Basically, these "rules" (and even the more objective statistical tests) are oversimplifications; they do not excuse YOU from understanding what is required to prove the point that you are trying to make.

# Statistical significance of the periodogram

e. For the periodogram, the following statistics apply to assess whether a peak of power density  $P_i$  is higher than expected from a white noise spectrum:

	90% CI	95% CI
Upper Bound	$19 P_i$	$39 P_i$
Lower Bound	$0.33 P_i$	$0.21 P_i$

**Obviously these limits are not very good!** If we are to see more subtle characteristics of the spectrum, it is necessary to improve these statistics.

# Daniell Estimator

Estimating a spectrum using a smoothing window (Daniell Estimator)

As with most collections of numbers, we can improve error bounds by averaging (at the expense of detail). In a power spectrum, we can average adjacent frequency bands at the expense of frequency resolution.

Several methods have been proposed to accomplish this averaging; for most geophysical time series, the simplest is adequate: the Daniell Estimator:

$$\overline{P}_j = \sum_{k=-n}^{k=+n} \frac{P_{j+k}}{2n+1}$$

(Note: in order to keep the spectrum frequency bands the same as the periodogram bands when averaging even numbers of bands, it is common to add the  $n-1$  bands on either side of the central band, and add  $1/2$  of the bands on either side of these  $n-1$  bands).

# Statistical significance of Daniell Estimator

"Equivalent Degrees of Freedom" (EDF)  $r = 2n$  where  $n = \#$  of periodogram bands included in average.

## Chi-square table

$\gamma$

$r$	0.025	0.05	0.95	0.975
2	0.051	0.103	5.991	7.378
4	0.484	0.711	9.488	11.143
6	1.237	1.635	12.592	14.449
8	1.690	2.733	15.507	17.535

—

$$\text{Bound} = (r/\gamma) P_j$$

# Example

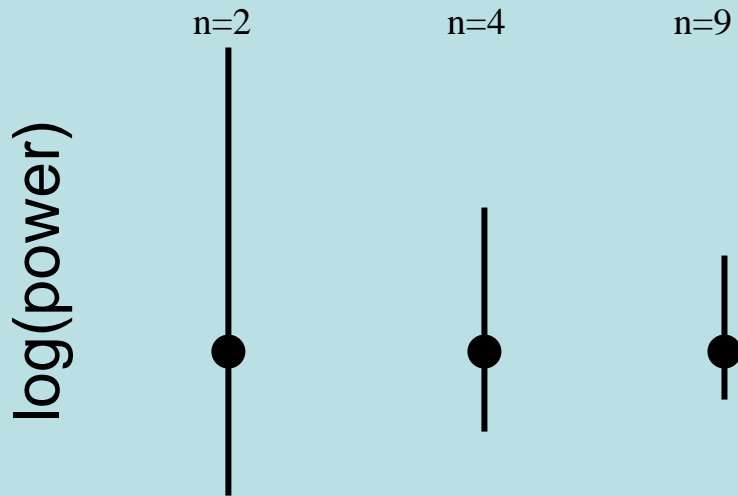
Example: suppose 2 periodogram bands are averaged ( $r=4$ ) and we want to know the upper and lower bounds that must be exceeded to define a spectral peak at the 95% confidence interval:

$$\text{The upper bound is : } \overline{4/.484 P_j} = 8.3 \overline{P_j}$$

$$\text{The lower bound is : } \overline{4/11.143 P_j} = 0.36 \overline{P_j}$$

The statistics of these bounds roughly goes as the square root of  $n$ , i.e. similar to counting statistics

(2) Since the bounds are multiplicative, error bars are fixed on a log-scale diagram:



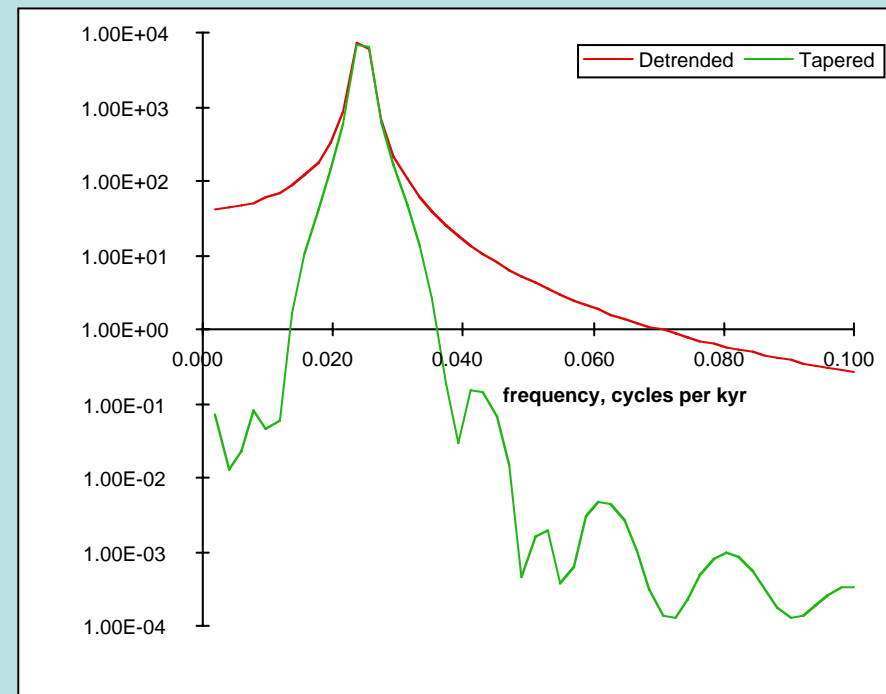
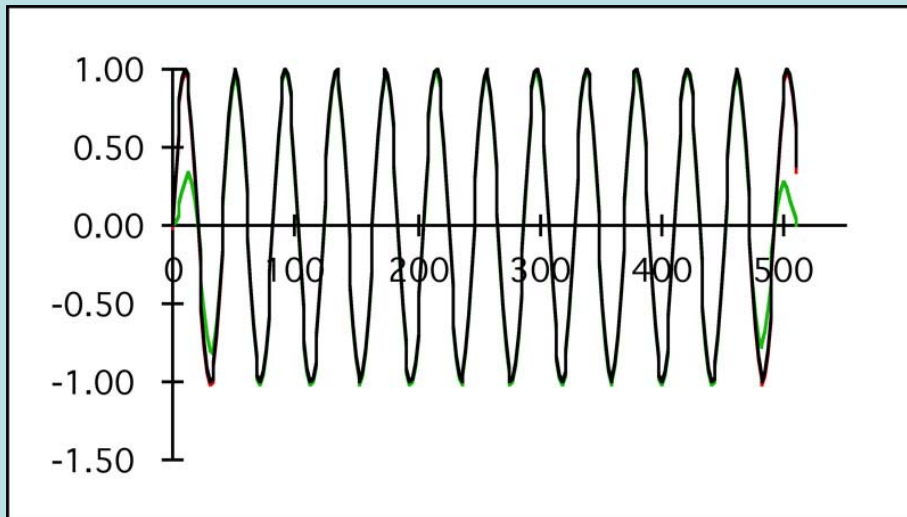
# The problem of frequency resolution

From the definition of the Fourier bands, it is obvious that resolution is poor for periods that are only a few multiples of the record length. What are you to do if you want a higher resolution spectrum? The safe answer is: Don't try to cheat mathematics: get a longer record! There is a more dangerous alternative, however. Suppose you then add a string of trailing zeros equal in number to the number of measurements. In effect, you have doubled the length of your time series without having added any data! While this may worry you, it doesn't bother the Fourier Transform at all, which will still happily compute the spectra. And it doesn't work too badly: in a test case where two sine waves corresponding to adjacent frequency bands in an original time series had the resolution doubled this way, the new FFT in fact was able to resolve the two sine frequencies. However, in doing so, it also generated "side bands" with significant amplitudes. So the extra resolution of these two bands was obtained at the expense of "contaminating" the rest of the spectrum. So in a real time series with a few strong frequency peaks, this method will compromise your ability to look at the rest of the spectrum. Caveat FFTer!

# Optimal Spectral Estimation

Tapering results in some loss of spectral power (most severe at low frequencies) and (in some cases) loss of resolution between frequency bands. But it also minimizes "leakage", the tendency for spectral power to "leak" from one frequency into the estimate for adjacent frequencies.

Example: a pure 41 kyr sine wave sampled 256 times during 510 kyr :



Note that the detrended (nearly raw) time series shows spectral power at either side of the actual frequency which "isn't really there". Tapering improves this situation, but does not eliminate all of the side-bands.

# Optimal Spectral Estimation

This observation leads to a concern over "optimal spectral estimation"

The simple Fourier transform/periodogram method described below works reasonably well for simple situations where a small number of well-separated dominant frequencies are present, and where you are only interested in dominant power at the dominant frequencies and not at the true weak power in the gaps between the dominant frequencies.

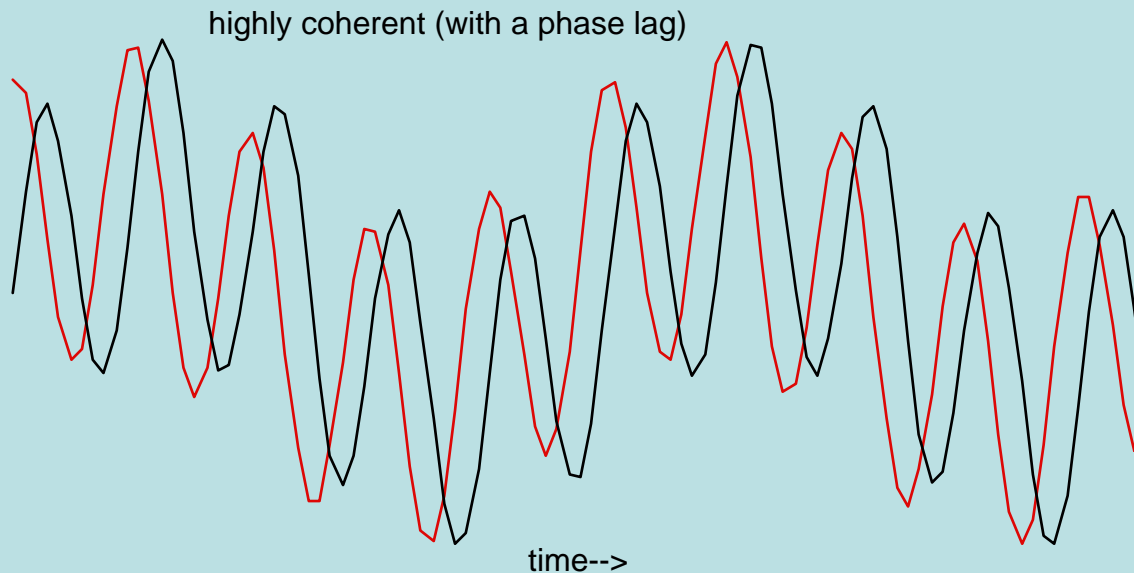
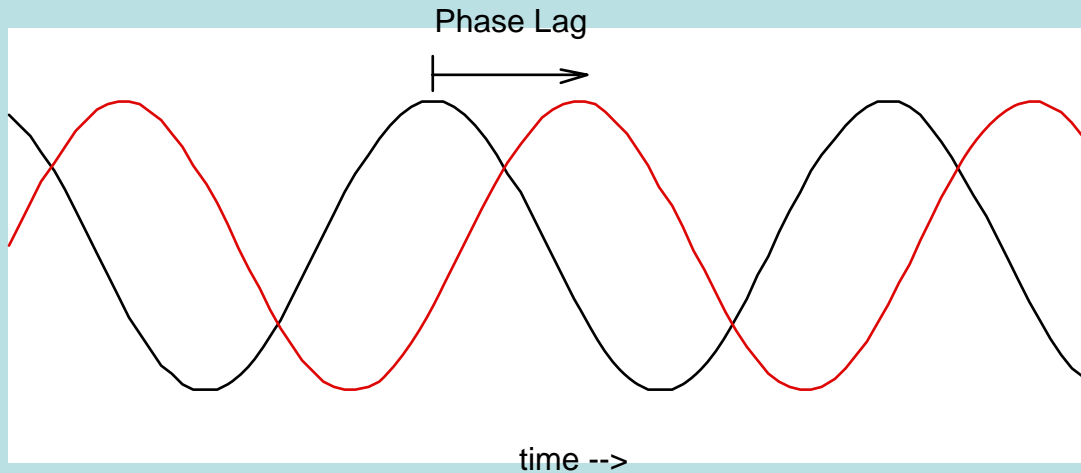
In other situations, where you really care about extracting the best possible estimate of the true spectrum, you must move on to other techniques. Arguments have raged over optimal spectral estimation, but it seems that the winner is David Thompson, who has shown that the best approach is to use a "multi-taper" strategy in which the averaged Fourier transforms (from independent spectra computed using a set of "eigentapers") are used to retain as much information as possible. [Actually what he says is : "...spectral estimates based on the simple periodogram or unwindowed FFT (or equivalently, on sample autocorrelations) including indirect estimates (also known as Blackman-Tukey (1958) estimates) or worse, adding misfit to bias, the autoregressive or 'maximum-entropy' estimates, must be considered both obsolete and extremely dangerous." (Thompson, 1990)]. This approach is beyond the limits of this course, but it is the right thing to do if you must have the best spectra.

# Coherence and Phase

- How well do two time series resemble each other (as a function of frequency)?

Coherence = “Correlation coefficient in frequency space” - a number varying between 0 and 1

- What are the *phase relationships* of the two time series?



# Calculating the cross-spectrum, coherence, and phase

Given two 'records' (X,Y) each has a power spectrum

$$a^2 + b^2 = (a + ib)(a - ib)$$

(i.e., the power spectrum is the complex conjugate of the Fourier coefficients)

$$\Phi_X(S) = \sum X(S) X^*(S)$$

$$\Phi_Y(S) = \sum Y(S) Y^*(S)$$

(where \* denotes complex conjugate; both  $\Phi_X(S)$  and  $\Phi_Y(S)$  are real and  $> 0$ )

3. The cross-spectrum  $\Phi_{XY}$  is similarly defined:

$$\Phi_{XY} = \sum X(S) Y^*(S)$$

$$(a_j + ib_j)(c_j - id_j) = a_j c_j + b_j d_j - (a_j d_j - c_j b_j)i$$

$$= C + iQ \text{ (a complex number)}$$

# Calculating the cross-spectrum, coherence, and phase

Coherence is the normalized cross-spectrum (the cross-spectral power normalized to the power of the two series)

$$\text{coh} = \frac{\Phi_{xy}}{(\Phi_x \Phi_y)^{1/2}} = C + iQ \text{ (a complex number)}$$

$$0 \leq \text{coh}(x,y) \leq 1$$

a. Band-averaging must be done (same definition as Daniell estimator), except that when computing phase, you must band-average the complex numbers before computing phase (think of the beating of nearby frequencies...). This is done as complex addition of vectors in the phase plane

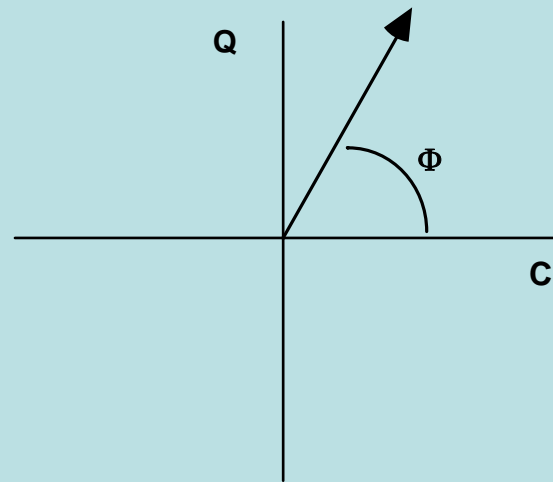
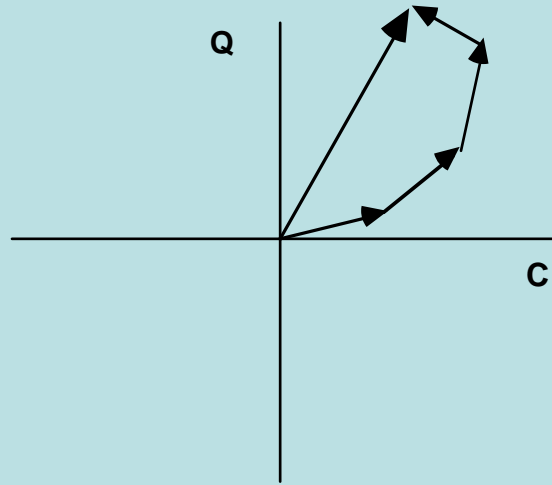
$$\text{coh} = \frac{\overline{C_2 + Q_2}}{\overline{P_1 P_2}}$$

$$\text{coherence magnitude} = (\overline{C_2 + Q_2})^{1/2}$$

phase

$$\varphi = \tan^{-1} (\overline{Q/C})$$

# Coherence and Phase on the complex plane:



# Example:

$$X: a_j + ib_j$$

$$Y: c_j + id_j$$

$$XY = (a+ib)(c-id)$$

$$a_j c_j + b_j d_j = C_j$$

$$b_j c_j - a_j d_j = Q_j$$

Then band-average  $C_j + iQ_j$  (Daniell estimator) on the complex plane

Coherence

Phase

1. cross-spectrum

1. cross-spectrum

2. compute coherence

2. band-average

3. Avg  $\rightarrow$  coherence

3. Compute phases

# Statistical significance of coherence and phase

Coherence: critical values for the test of hypothesis  $q=0$

n	95% CI	90% CI
2	0.975	0.948
3	0.881	0.827
4	0.795	
5	0.726	0.662
6	0.671	
7	0.627	
10	0.533	0.475

However, these statistics only apply to time series where the time scales are precisely accurate. Paleoclimatic time series are often "tuned" to match orbital variability - in this case the coherence between orbital parameters and the coherence of the tuned time series is falsely elevated and isn't a particularly useful statistic.

## b. Phase

$$\text{error} = \arcsin \left[ \left[ \frac{1 - \text{coh}^2}{\text{coh}^2(2n-2)} \right]^{1/2} t_{2n-2}(\alpha/2) \right]$$

where  $t$  is the t-statistic and  $\alpha$  is the desired confidence level, i.e. for 95% CI,  $\alpha = 1-.05$ .

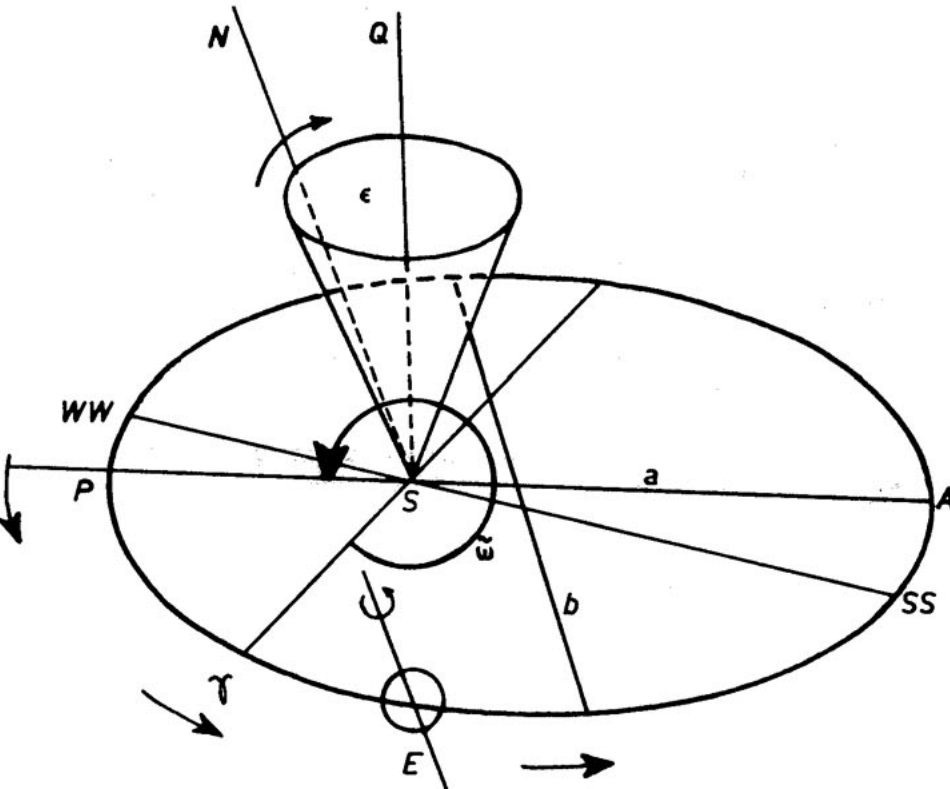
# Frequency Filtering of Time Series

Suppose you would like to “filter out” the signal within a band of frequencies. There are several ways this can be done; the simplest is: Fourier Transform the data, multiply the coefficients by multipliers (ranging from 0 to 1), and then perform the Inverse Fourier Transform.

(warning: multipliers should change slowly in adjacent bands; i.e. don't go from 0 to 1 in adjacent bands)

# Elements of the Earth's Orbit

(Berger, 1981)



Elements of the earth's orbit. The orbit of the Earth E, around the Sun S is represented by the ellipse P  $\gamma$  E A, P being the perihelion and A the aphelion. Its eccentricity  $e$ , is given by  $(a^2 - b^2)^{1/2} / a$ ,  $a$  being the semimajor axis and  $b$  the semiminor axis. WW and SS are respectively the winter and the summer solstice,  $\gamma$  is the vernal equinox; WW, SS and  $\gamma$  are located where they are today. SQ is perpendicular to the ecliptic and the obliquity,  $\epsilon$ , is the inclination of the equator upon the ecliptic, i.e.  $\epsilon$  is equal to the angle between the earth's axis of rotation SN and SQ.  $\omega$  is the longitude of the perihelion relatively to the moving vernal equinox and is equal to  $\Pi + \psi$ . The annual general precession in longitude,  $\psi$ , describes the absolute motion of  $\gamma$  along the earth's orbit relative to the fixed stars.  $\Pi$ , the longitude of the perihelion, is measured from the reference vernal equinox of 1950 A.D. and describes the absolute motion of the perihelion relatively to the fixed stars. For any numerical value of  $\omega$ ,  $180^\circ$  is subtracted for a practical purpose: observations are made from the Earth, and the Sun is considered as revolving around the Earth.

# Summary: orbital influence on insolation at the top of the atmosphere

- These changes in the earth's orbital elements affect radiation received at the top of the atmosphere ("insolation") as a function of hemisphere, latitude, and time of year.

Effect of precession/eccentricity:

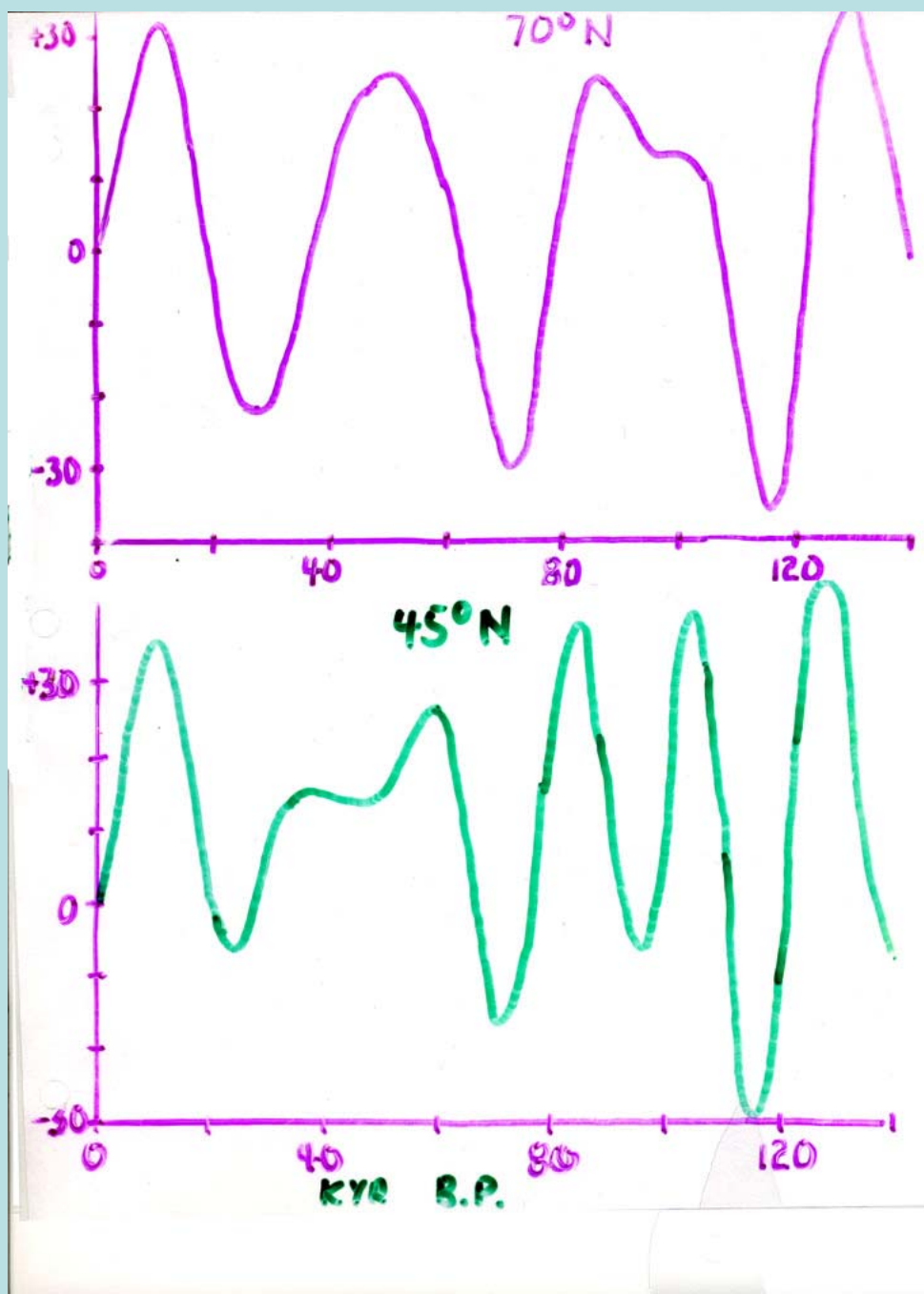
Inter-hemispheric radiation receipt: the hemisphere whose summer occurs during perihelion receives more insolation than the other hemisphere). The higher the eccentricity, the stronger the contrast.

Seasonal contrast within a hemisphere: as a hemisphere alternates between periods of summer perihelion and winter perihelion, the seasonal contrast in insolation is modified. The two hemispheres are out of phase with respect to this effect.

Effect of obliquity: high-latitude summer insolation: high tilt leads to more radiation received at high latitudes during summer (that comes at the expense of the mid- and low-latitudes; high-latitude winters not affected by changes in tilt).

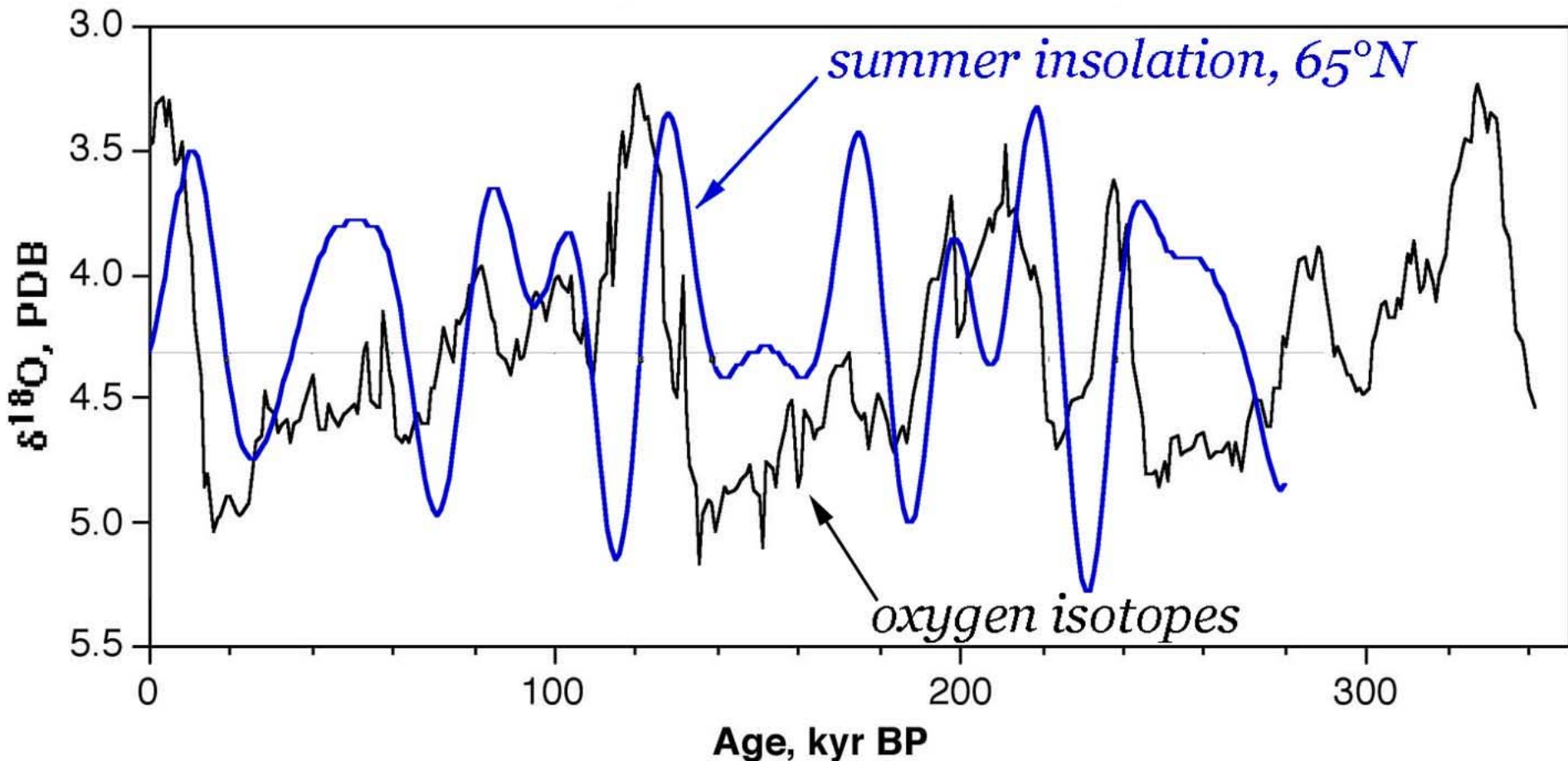
- These orbital characteristics can all be calculated accurately via Newtonian mechanics into the distant past (many millions of years). Accumulation of uncertainties (e.g. in relative masses of planets; shape and density distribution of planets) causes absolute values (i.e., which side of the sun is the earth on at some exact point in time in the future?) to be uncertain beyond several million years, although the frequencies are probably known reasonably well beyond that time. For the last million years, we may regard these calculations as virtually unquestionable.

Summer half-year insolation, cal/cm<sup>2</sup>/day



Integrated over a half-year centered on summer, obliquity dominates high latitude insolation and precession dominates lower latitude insolation

# Oxygen isotopes compared to summer insolation at 65°N



# Computation of the Fourier Transform

Accepting the truth of the theorem, the discrete Fourier Transform is just an application of simultaneous equations. For discrete uniformly-sampled data, we are taking  $N$  observations of  $G(t)$  from  $t_1$  to  $t_N$  [whose record length (period) is  $P=t_N-t_1$ ] and the spacing between samples is  $\Delta t=P/(N-1)$ ] and converting to  $N/2$  pairs of sine and cosine coefficients. The number of coefficients is equal to the number of observations, so this is an exercise in solving a system of  $N$  simultaneous equations. Let  $\mathbf{A}$  = an  $N \times N$  square array of the sine and cosine time series for each of the harmonics, where each row  $n$  of the array (for  $j= 0$  to  $N-1$ ) is:

$$\begin{matrix} \sin(2\pi j\Delta t) & \cos(2\pi j\Delta t) & \sin(4\pi j\Delta t) & \cos(4\pi j\Delta t) & \sin(6\pi j\Delta t) & \cos(6\pi j\Delta t) & \dots & \sin(2\pi(N/2) j\Delta t) & \cos(2\pi(N/2) j\Delta t) \end{matrix}$$

e.g.:

$$\mathbf{A} = \begin{bmatrix} \sin(2\pi/N 0*\Delta t) & \cos(2\pi/N 0*\Delta t) & \sin(4\pi/N 0*\Delta t) & \cos(4\pi/N 0*\Delta t) & \dots & \sin(2\pi(N/2) 0*\Delta t) & \cos(2\pi(N/2) 0*\Delta t) \\ \sin(2\pi/N 1*\Delta t) & \cos(2\pi/N 1*\Delta t) & \sin(4\pi/N 1*\Delta t) & \cos(4\pi/N 1*\Delta t) & \dots & \sin(2\pi(N/2) 1*\Delta t) & \cos(2\pi(N/2) 1*\Delta t) \\ \dots & \dots & \dots & \dots & \dots & \dots & \dots \\ \sin(2\pi/N (N-1)\Delta t) & \cos(2\pi/N (N-1)\Delta t) & \sin(4\pi/N (N-1)\Delta t) & \cos(4\pi/N (N-1)\Delta t) & \dots & \sin(2\pi(N/2) (N-1)\Delta t) & \cos(2\pi(N/2) (N-1)\Delta t) \\ \dots & \dots & \dots & \dots & \dots & \dots & \dots \end{bmatrix}$$

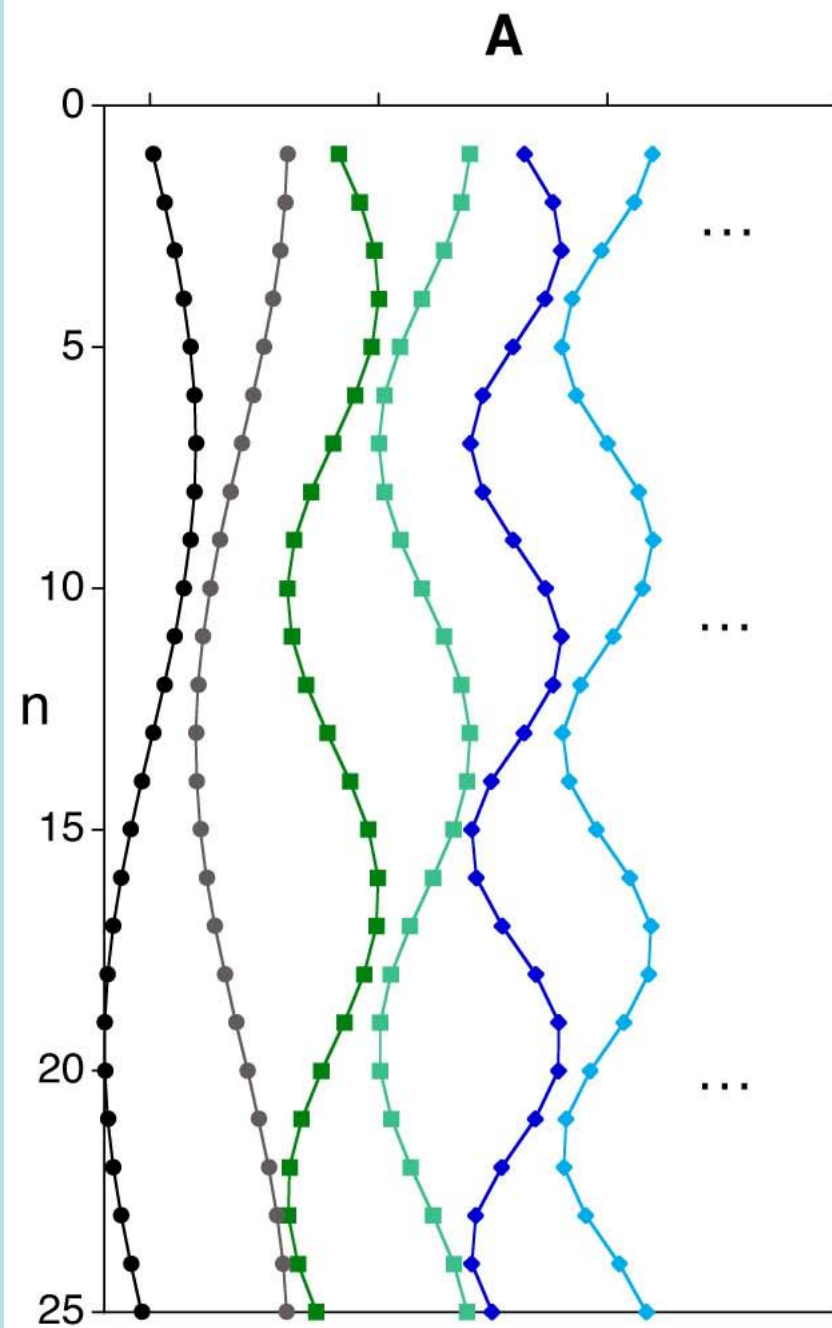
and let  $\mathbf{x}$  = an  $N \times 1$  vector of the Fourier coefficients (a, b) arranged vertically:

$$\mathbf{x} = \begin{bmatrix} a_1 \\ b_1 \\ a_2 \\ b_2 \\ \dots \\ a_{N/2} \\ b_{N/2} \end{bmatrix}$$

and let  $\mathbf{g}$  = an  $N \times 1$  vector of the discrete observations of  $G(t)$ :

$$\mathbf{g} = \begin{bmatrix} g(t_1) \\ g(t_2) \\ g(t_3) \\ g(t_4) \\ \dots \\ g(t_{N-1}) \\ g(t_N) \end{bmatrix}$$

So:  $\mathbf{Ax} = \mathbf{G}$



**x**

**=**

**g**

$a_1$

$b_1$

$a_2$

$b_2$

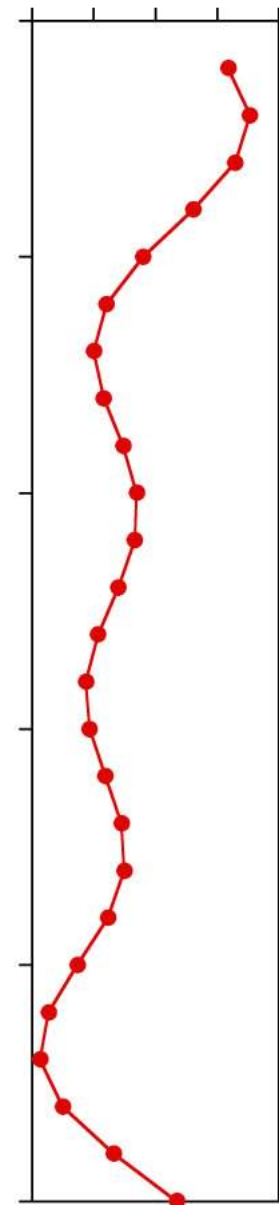
$a_3$

$b_3$

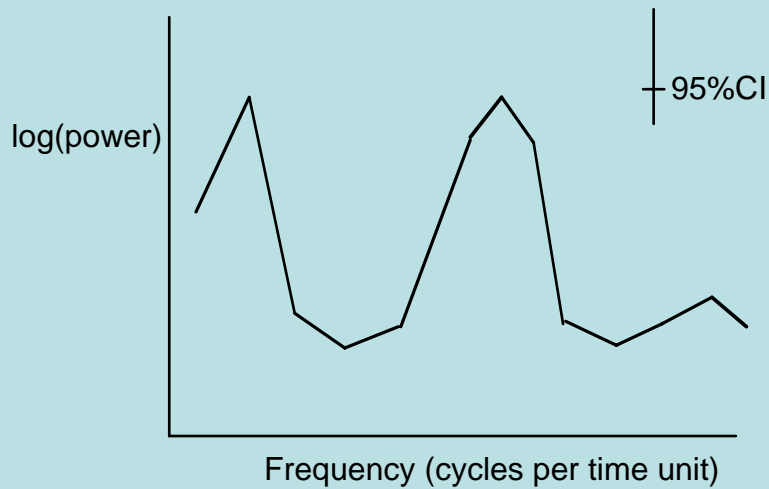
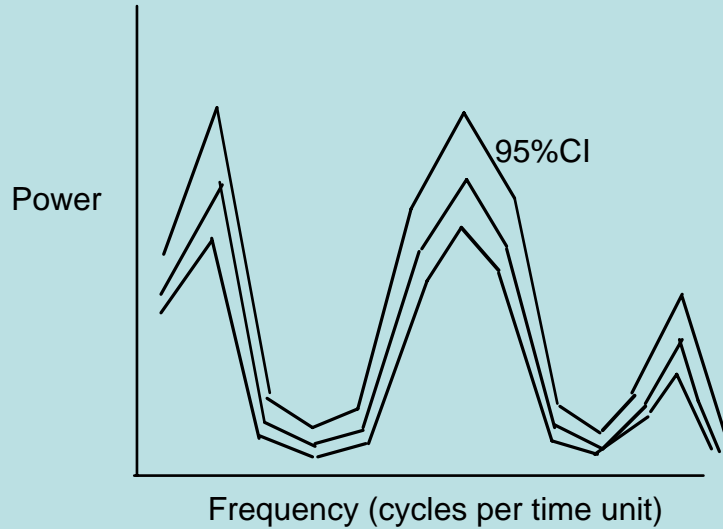
...

$a_{N/2}$

$b_{N/2}$



# Periodogram



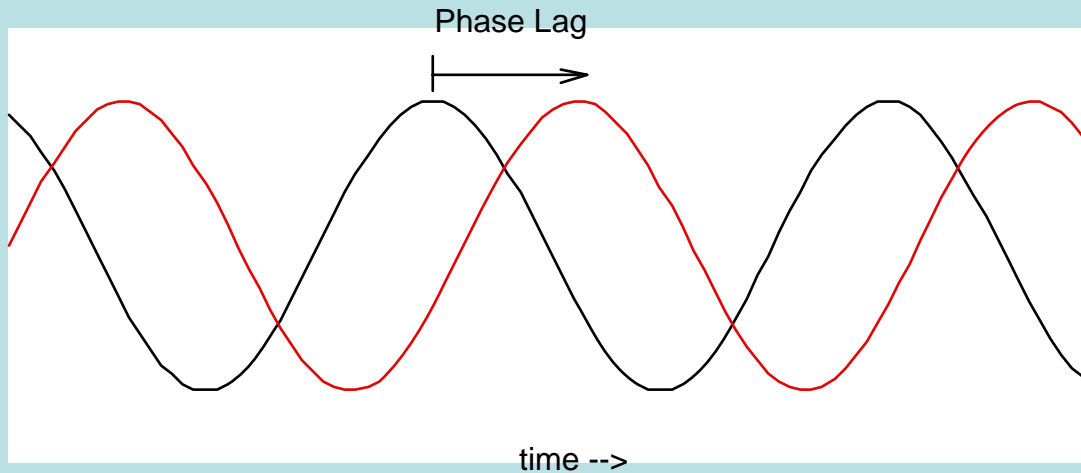
The periodogram is a plot of power or  $\log_{10}(\text{power})$  vs/ frequency, which is evenly spaced for the Fourier Transform

# Coherence and Phase

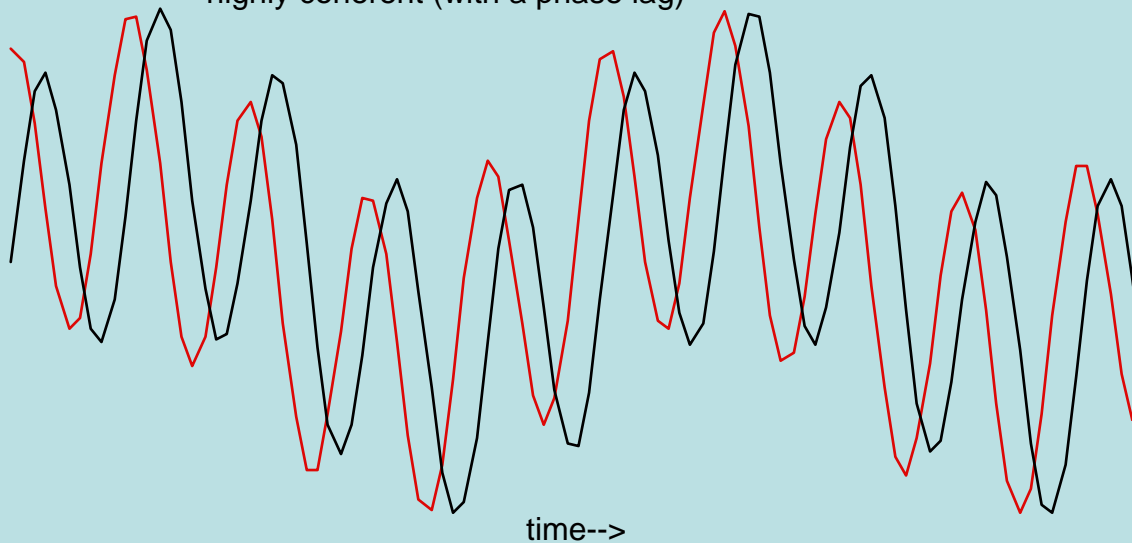
- How well do two time series resemble each other (as a function of frequency)?

Coherence = “Correlation coefficient in frequency space” - a number varying between 0 and 1

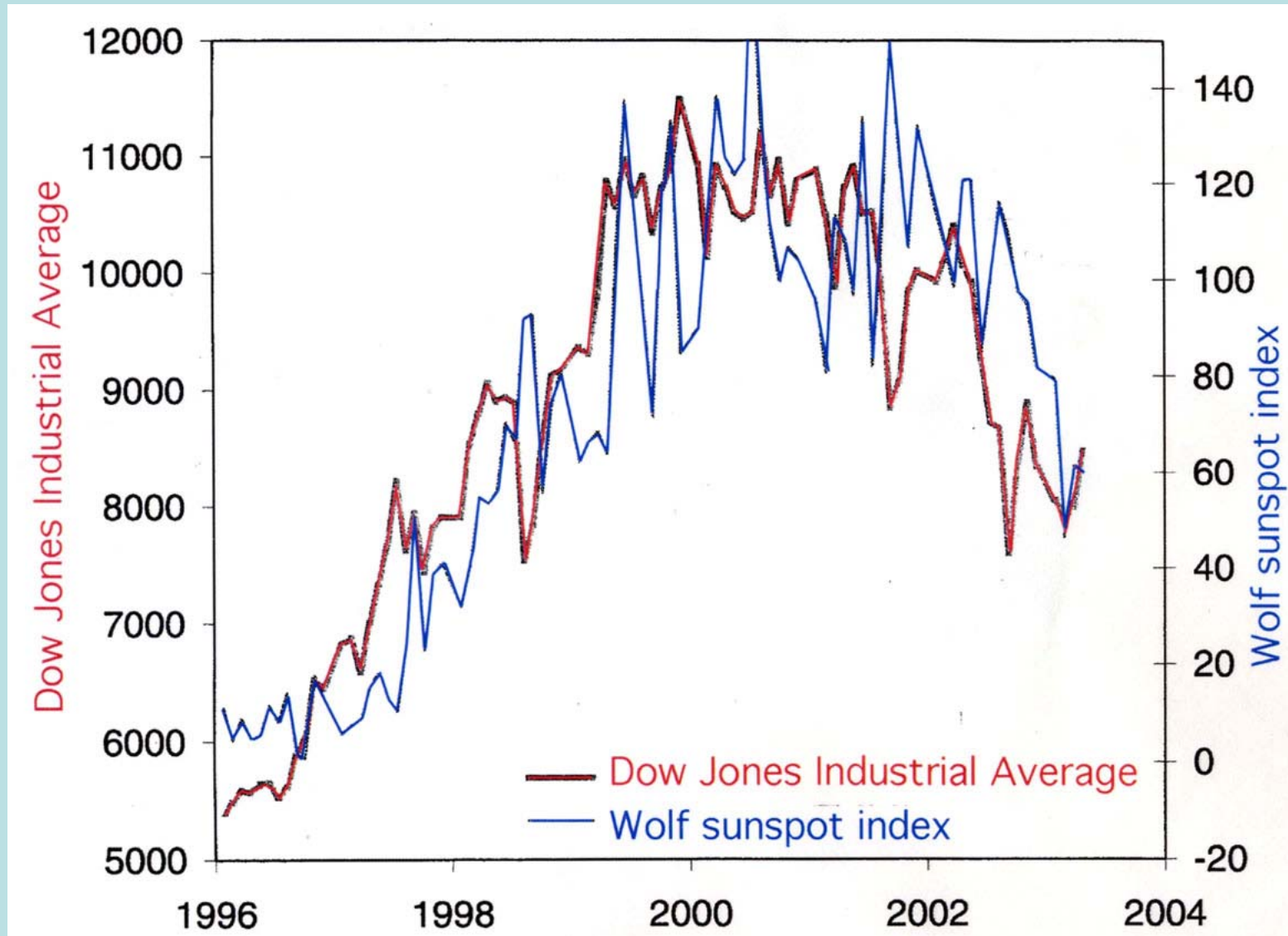
- What are the *phase relationships* of the two time series?



highly coherent (with a phase lag)



# *Correlation does not require Causation*



Images removed due to copyright restrictions.

Hays, Imbrie, & Shackleton (1976)

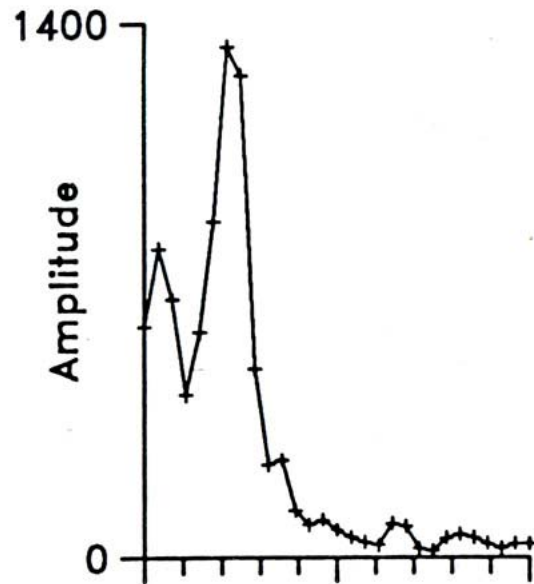
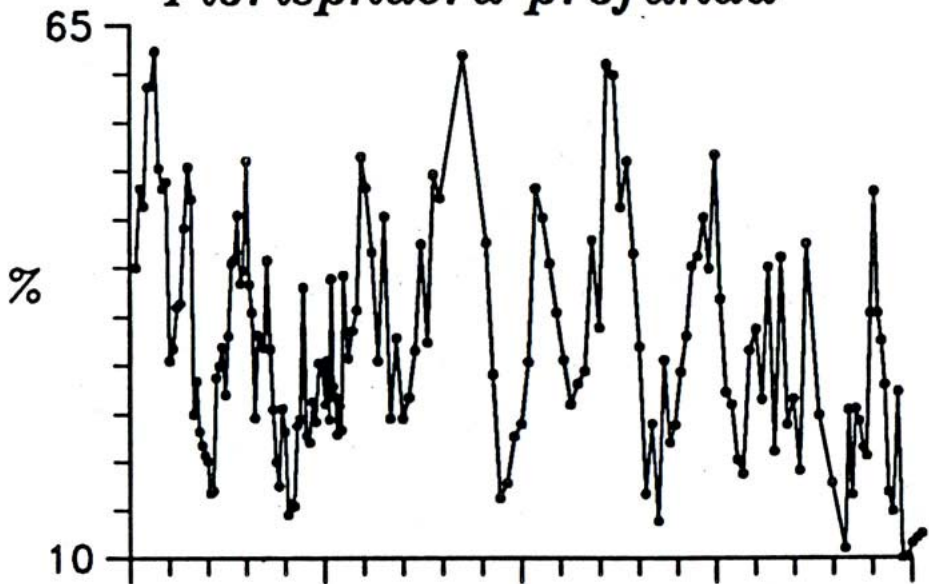
## Hays, Imbrie and Shackleton (1976) outline:

- Start with time scale derived from V28-238 linear depth interpolation from B-M magnetic reversal (730 ka) (supported by radiometric dates from Barbados terraces).
- Spectral analyses of  $\delta^{18}\text{O}$ , radiolaria seem to indicate peaks at orbital frequencies (precession, obliquity, eccentricity)
- Use frequency filtering to examine phase relationships; note that phases are consistent for the radiometrically-dated interval but diverge for the preceding period.
- ASSUME that the phase divergence is due to errors in the time scale, TUNE the time scale to get consistent phases.

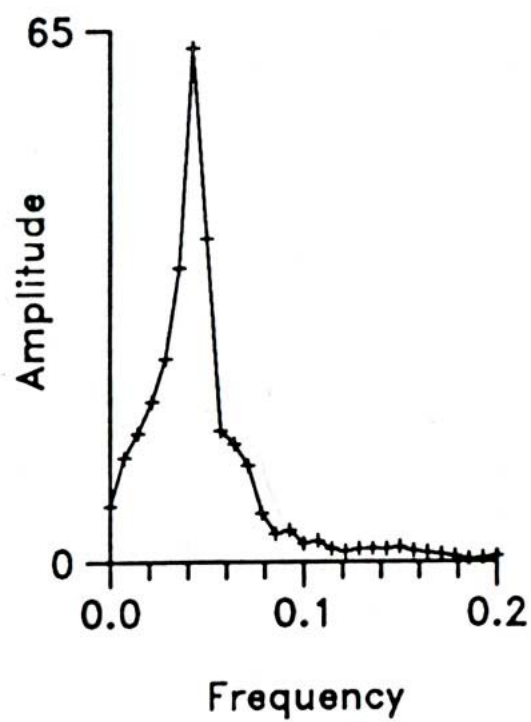
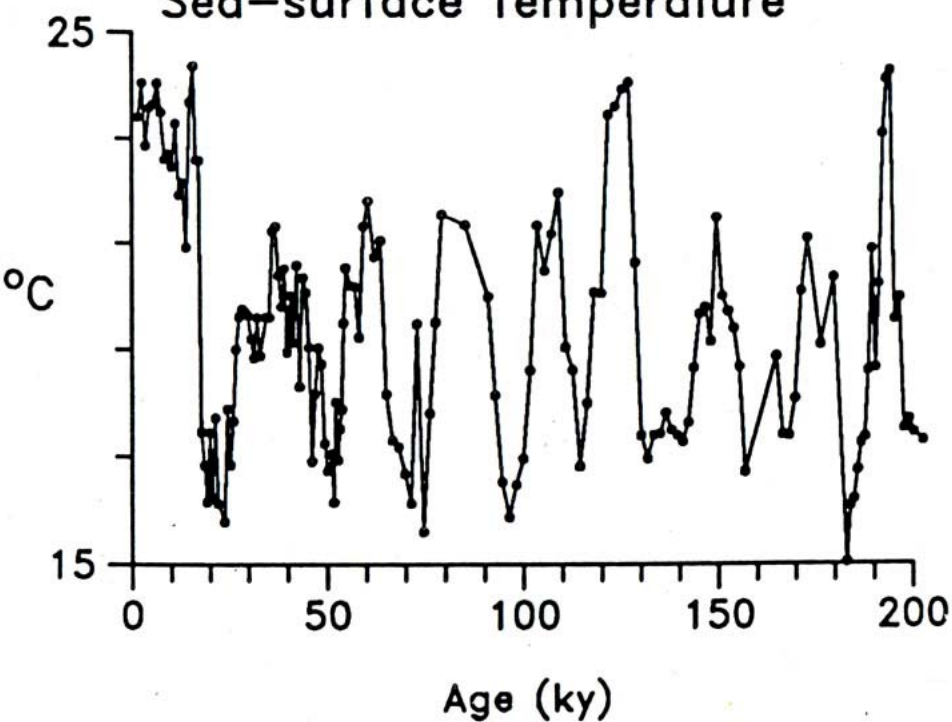
Image removed due to  
copyright restrictions.

Evans and Freeland (1977)  
Science 198:528-530

*Florispheera profunda*



Sea-surface Temperature



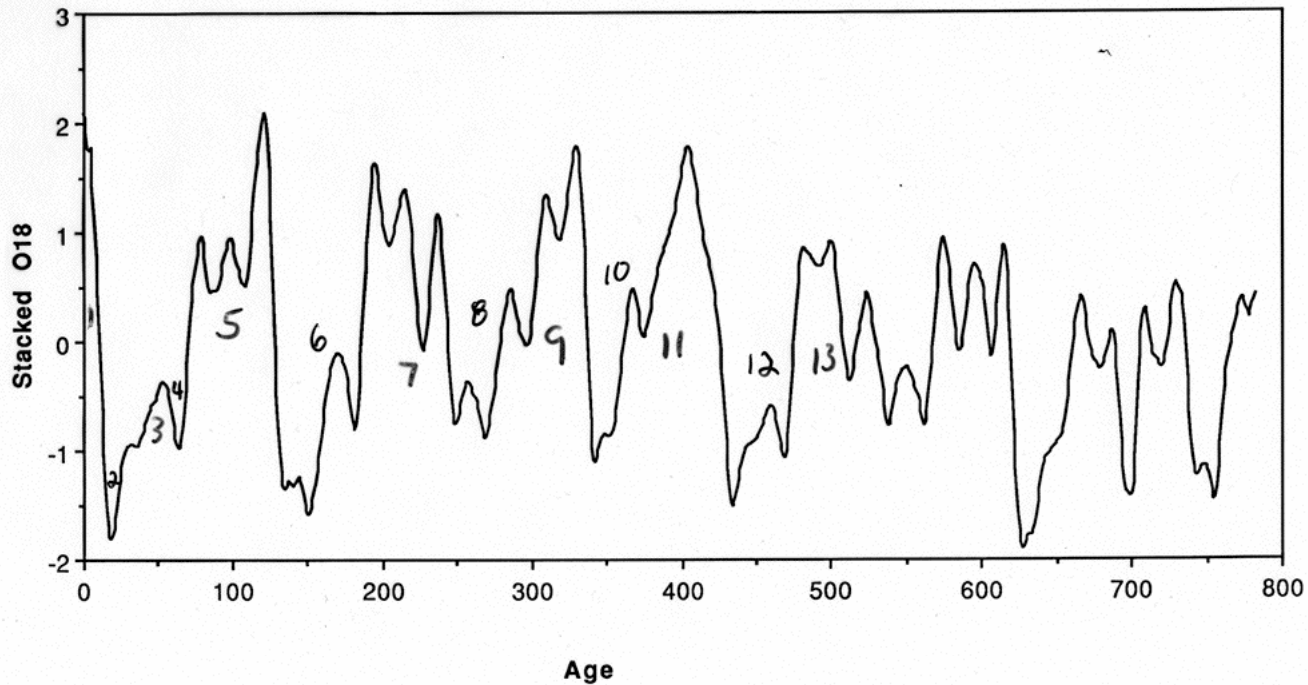
Molfino (1980)  
tropical Atlantic

Imbrie and Imbrie  
orbit->ice volume model

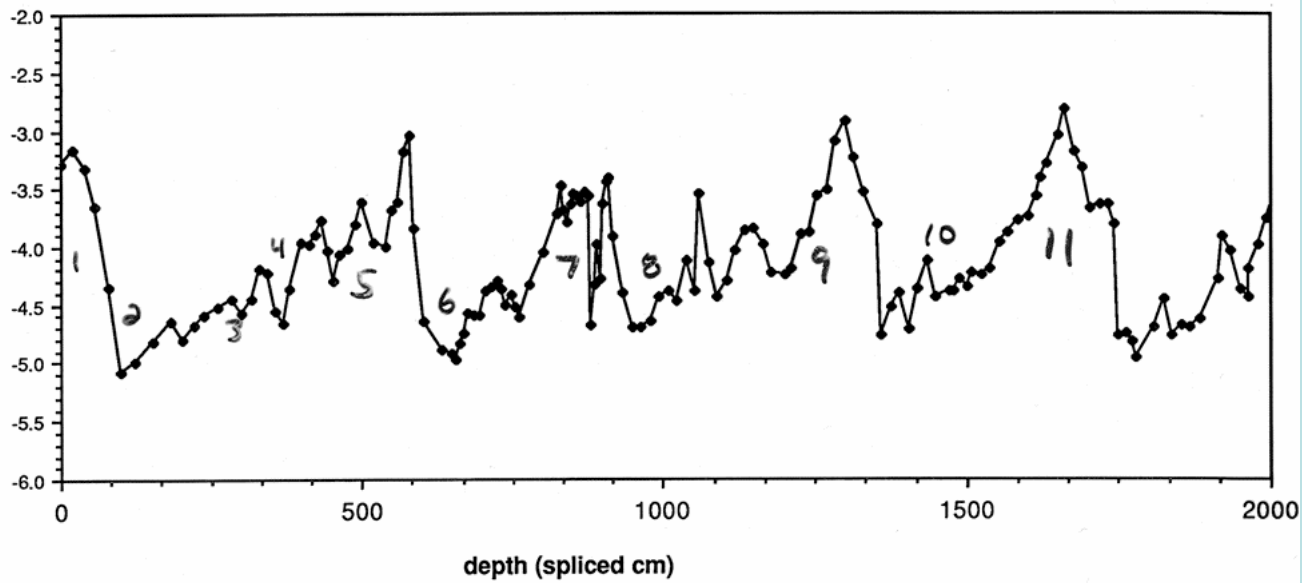
Image removed due to copyright restrictions.

Bassinot et al. (1994)  
EPSL 126:91-108

# SPECMAP STACK



ODP 607 composite



# SPECMAP phase wheel

## ORBITAL FRAMEWORK OF THE SPECMAP PHASE WHEEL

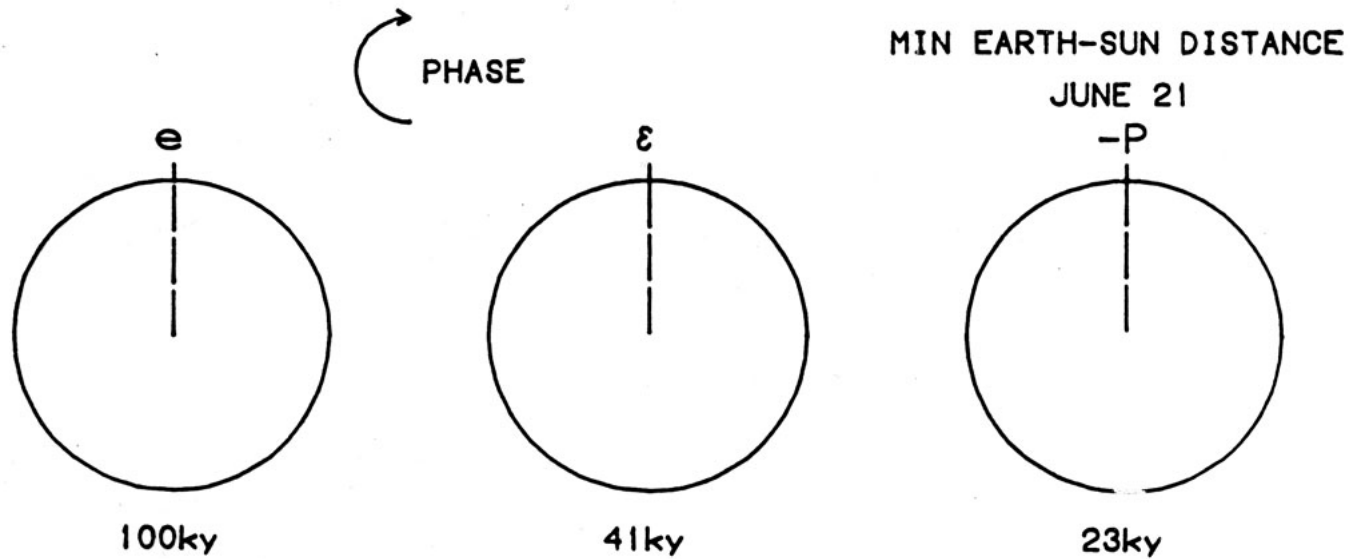


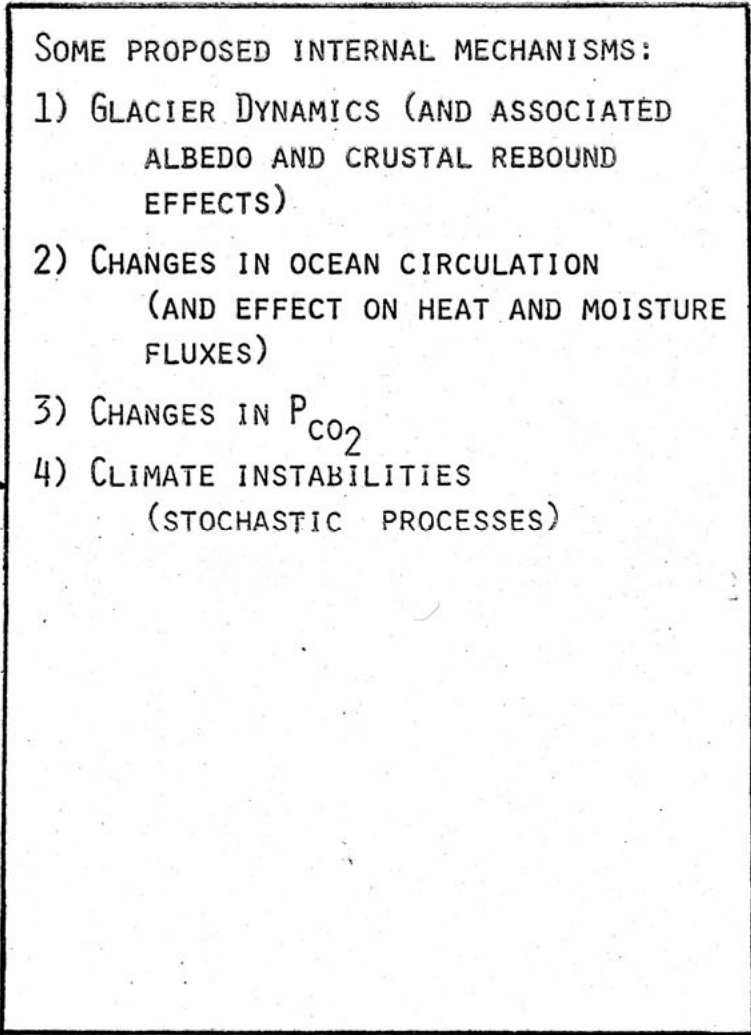
Fig. 2. Conventions of the SPECMAP phase wheel. Cyclical changes in orbital geometry for the 100-ky eccentricity cycle ( $e$ ), the 41-ky obliquity cycle ( $\epsilon$ ), and the 23-ky precession-index cycle ( $P$ ) are represented by vectors rotating clockwise (+) on phase dials. Zero phase on each dial is defined as the position of a vector pointing to the top of the page, and is arbitrarily defined as maximum  $e$ , maximum  $\epsilon$ , and June 21st perihelion ( $-P$ ). These definitions correspond to orbital geometries that are empirically associated with forcing toward interglacial conditions. Except for  $\epsilon$ , however, there is no a priori physical basis for assuming that these geometries actually represent the maximum interglacial forcing.

Images removed due to copyright restrictions.

Imbrie et al. (1992)



ORBITAL INPUT  
(INSOLATION VARIATIONS)



CLIMATE OUTPUT  
( $\delta^{18}O$ )

# Reading

Baksi A. K., Hsu V., McWilliams M. O., and Farrer E. (1992)  $^{40}\text{Ar}/^{39}\text{Ar}$  dating of the Brunhes-Matuyama boundary and the Pleistocene geomagnetic polarity timescale. *Science* 256, 356-357.

Bassiot, F. C., L. D. Labeyrie, et al. (1994). "The astronomical theory of climate and the age of the Brunhes-Matuyama magnetic reversal." *Earth Planet. Sci. Lett.* 126: 91-108.

Berger A. L. (1981) The astronomical theory of paleoclimates. In *Climatic Variations and Variability: Facts and Theories* (ed. A. Berger) pp. 501-538. Reidel

Koopmans, L.H., *The Spectral Analysis of Time Series*, Academic Press, New York, 1974. [This book is somewhat difficult reading in parts, but it contains all of the relevant formulae and statistical tables, as well as examples].

\*Hays, J.D., J. Imbrie, and N. Shackleton (1976) Variations in the earth's orbit: pacemaker of the ice ages, *Science* 194:1121-1132.

\*Imbrie, J. et al. (1984) The orbital theory of Pleistocene climate: support from a revised chronology of the late marine  $\delta^{18}\text{O}$  record, in *Milankovitch and Climate*, (ed. A. Berger et al.), D. Reidel ~Press, Hingham, Mass.

Imbrie, J., et al. (1992). "On the structure and origin of major glaciation cycles 1. Linear responses to Milankovitch forcing." *Paleoceanogr.* 7: 701-738.

Imbrie, J., et al. (1993). "On the structure and origin of major glaciation cycles 2: the 100,000-year cycle." *Paleoceanogr.* 8: 699-736.

Imbrie, J., A. McIntyre, et al. (1989). Oceanic response to orbital forcing in the late Quaternary: observational and experimental strategies. *Climate and Geosciences*. A. Berger and e. al. Netherlands, Kluwer: 121-164.

Martinson, D. G., N. G. Pisias, et al. (1987). "Age dating and the orbital theory of the ice ages: development of a high-resolution 0 to 300,000 years chronostratigraphy." *Quat. Res.* 27: 1-29.

Raymo M. E., Ruddiman W. F., Martinson D. G., Clement B. M., and Backman J. (1989) Late Pliocene variation in Northern Hemisphere ice sheets and North Atlantic Deep Water circulation. *Paleoceanogr.* 4, 413-446.

Ruddiman, W. and A. McIntyre (1981) Oceanic mechanisms for amplification of the 23,000 year ice volume cycle, *Science* 212: 617-627.

Shackleton, N.J. and N.G. Pisias (1985) Atmospheric carbon dioxide, orbital forcing, and climate, in *The Carbon Cycle and Atmospheric CO<sub>2</sub>: Natural Variations Archean to Present* (eds. E.T. Sundquist and W.S. Broecker), *Am. Geophys. Union*, pp.303-318.

Shackleton, N. J., A. Berger, et al. (1990). "An alternative astronomical calibration of the lower Pleistocene timescale based on ODP site 677." *Trans. Royal Soc. Edinburgh: Earth Sci.* 81: 251-261.

Spell, T.L. and I. McDougall (1992) Revisions to the age of the Brunhes-Matuyama boundary and the pleistocene geomagnetic polarity timescale

Tauxe L., Herbert T., Shackleton N. J., and Kok Y. S. (1996) Astronomical calibration of the Matuyama-Brunhes boundary: Consequences for magnetic remanence acquisition in marine carbonates and the Asian loess sequences. *Earth Planet. Sci. Lett.* 140, 133-146.

Thompson, D. (1990) Quadratic-inverse spectrum estimates: applications to paleoclimatology, *Phi. Trans. R. Soc. Lond. A* 332:539-537.

Tiedemann R., Sarnthein M., and Shackleton N. J. (1994) Astronomic timescale for the Pliocene Atlantic  $\delta^{18}\text{O}$  and dust flux records of Ocean Drilling Program site 659. *Paleoceanogr.* 9, 619-638.

Did increasing Northern Hemisphere summer insolation cause the end of the last ice age?

